CALIFORNIA STATE UNIVERSITY, NORTHRIDGE

SEISMIC ANISOTROPY BENEATH THE AFRICAN PLATE

A thesis submitted in partial fulfillment of the requirements

For the degree of Master of Science in Geology,

Geophysics

By

Melissa Nunley

May 2013

The Thesis of Melissa Nunley is approved:

Dr. Doug Yule Date

Dr. Gerry Simila Date

Dr. Dayanthie Weeraratne, Chair Date

California State University, Northridge

Table of Contents

ABSTRACT

SEISMIC ANISOTROPY BENEATH THE AFRICAN PLATE

By

Melissa Nunley

Master of Science in Geology, Geophysics

The African continental plate is composed of a series of cratons and mobile belts with activation ages ranging from the present to the Archean. Although previous studies show the assembly of Africa has left behind a complex crust and lithospheric fabric, the style and timing of deformation is not well known. To study the degree and style of deformation of continental lithosphere during rifting and collisional events, I use seismic anisotropy to measure mineral alignment and strain accommodated by these tectonic events. Here I study seismic anisotropy beneath the African continent using instruments within the Africa Array and permanent Global Seismic Network stations located throughout Africa. I use SKS phases and shear wave splitting techniques for 28 teleseismic earthquake events. Stations located in the Ethiopian rift zone yield a NE-SW fast direction with the largest delay times of 1.5 s. One station (KOWA) located in the West African craton and three other stations located on the West African coast display a NW-SE fast direction and average delay times of 0.8 s. A group of stations located on Archean crust in central Africa skirt the Congo craton and display consistent NNE fast directions and delay times of 1.0 s. Two stations, LSZ and TEZI are located in the Damara suture belt between the Congo and Kaapvaal cratons display a NE-SW fast direction parallel to the suture axis. New stations available south of the Kaapvaal craton

reveal a NE fast direction with delay times that vary from 0.5 to 1.3 s. These results indicate that seismic anisotropy across the African continent is not uniform as might be suggested from absolute plate motion. Our results, however, do show consistent variations between cratonic regions and mobile belts. The delay times averaged over the cratonic regions is 0.67 s +/- 0.14 s and are significantly smaller than delay times observed in mobile belts of 1.4 s +/- 0.07 s. Comparison of the fast direction of anisotropy within cratons with current plate motion suggests that the majority of the splitting observations within cratons are due to remnant fossil fabric from previous collisional events and has very little contribution from sublithospheric mantle flow today. We suggest that repeated convergent and rifting events causes depletion and dehydration within a craton creating stronger, and stable lithosphere that is resistant to deformation during later collisional events. By contrast, mobile belts that are younger in age and more fertile are more readily deformed under large tectonic stresses. Remnant or ancient anisotropic fabric may thus be preserved in cratonic lithosphere where it is stored from previous collisions while mobile belts reflect the most recent tectonic events.

Chapter 1 Introduction

It has been proposed that the lithospheric mantle stores signatures of strain caused by previous tectonic events (Silver, 1996). Are these signatures characteristic of ancient historical events, or present day tectonics? The African continent is unique in that it is made up of over 5 distinct Archean continental cratons joined together by younger mobile belts. Other continents by comparison (see appendix Figure A2) generally have a single Archean cratonic core that have grown by accretion of Proterozoic and younger terranes into the large continental masses we observe today. The only exception is South America which was joined with Africa as part of the continent Atlantica (e.g. Rogers, 1996) until the south Atlantic rifting event ~80 Ma. Examination of seismic anisotropy and mantle fabric alignment can provide insights into of the behavior of the lithospheric mantle under stress (Silver, 1996; Silver and Chan, 1991). We will use seismic anisotropy measurements to determine whether the conditions of strain and stress are stored within these ancient cratonic blocks or whether they record present day tectonic activity.

Anisotropy is used to describe a medium whose elastic properties are functions of strain orientation (Silver, 1996). Shape preferred orientation is a type of fabric that develops due to shearing of a material that causes the formation of elongate or disc-like grains, grain aggregates, pore spaces, or melt pockets. In other cases, dislocations may form that move through the crystal lattice during dislocation creep due to applied stress. These changes produced in the crystal lattice are known as lattice-preferred orientation (LPO). Normally the orientation of minerals is random causing the magnitude of a uniform direction of anisotropy to be weak on average. As plates propagate or converge in one direction, mantle lithospheric material is deformed by drag or strain consequently producing alignment of mantle minerals (Appendix A1). Anisotropy in a fabric can form from several distinctive factors such as, fluid filled cracks, melt-filled cracks at mid-ocean ridges, the alignment of mantle minerals, or alternating anisotropic layers that maintain varying elastic properties (Silver, 1996). As a shear wave passes through an anisotropic medium the vertical and horizontal components become separated according to the direction of mineral alignment (Appendix Figure A2).

To measure and examine deformation throughout the African continent, I measure polarization anisotropy with SKS splitting techniques (Silver and Chan, 1991) using events recorded by the Africa Array and Global Seismic Networks. This technique allows anisotropy to be recorded on the receiver side and accurately measures the magnitude of deformation within the mantle. I will measure anisotropic values in each craton (where measurements are available) and its surrounding region. Our results indicate that seismic anisotropy is not uniform across the continent. This suggests that anisotropy is not a simple result of present day absolute plate motion (APM) but is produced and stored from previous tectonic events. Our results indicate that cratonic lithosphere is considerably stronger than the surrounding mobile belts. In the presence of the most recent tectonic events, mobile belts appear to accommodate strain deformation while cratonic lithosphere is resistant and remains intact. In addition, the stable cratonic lithosphere records uniform seismic anisotropic directions that are not consistent with present day plate motion and appears to record and preserve remnant fabric from ancient tectonic events.

1.1 Evolution of African Continent

The tectonic evolution of the African continent is complex and intricate (Figure 1). Africa is made up a series of continental cratons that have been assembled over several Wilson cycles. According to tectonic evolution theory (Rogers, 1996), Pangea was made up of three large masses that combined to form Pangea. These three initial continents are named: Ur, Artica, and Atlantica (Figure 2a). The oldest of the continents, Ur, formed around 3 billion years ago. This continent was comprised of the present day regions of the Kaapvaal craton, Pilbara region, and possibly Madagascar and India (Figure 2a). It was originally comprised of five different cratons: Pilbara craton, Kaapvaal craton, Bhandara craton and the Singhbhum craton (Figure 2a). Additional mobile belts and cratons were added to the continent during 3 Ga-1.5 Ga. Around 2.8-2.0 Ga, the observation of several major shear zones indicate collision of multiple cratonic sequences including the Limpopo belt that formed from the collision between Zimbabwe and Kaapvaal cratons, the Lurio and Namama belts that formed during the Grenville to Pan-African time, the Satpura and Copper belt which formed during the Proterozoic time period, and the Capricorn orogen active around 2.1 Ga. Ur is suggested to have expanded around 1.5 Ga to the size shown due to further accretion to the mobile belts (refer to Appendix Figure A4).

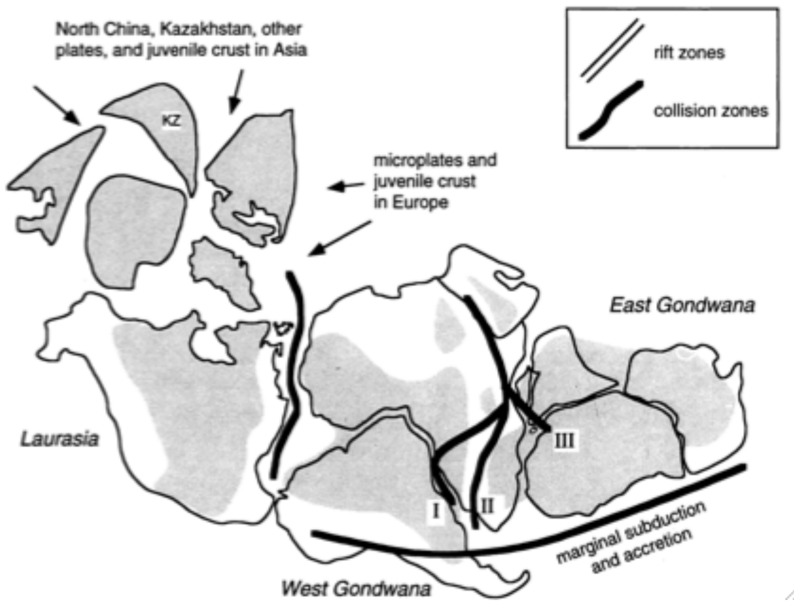

Figure 1: Assembly of the super continent Pangea. Solid black lines represent collisional zones. Gray regions indicate land mass location during collisional event. White enclosed regions indicate the relation of present day continents to continents present during assembly (Rogers, 1996).

.

A) B)

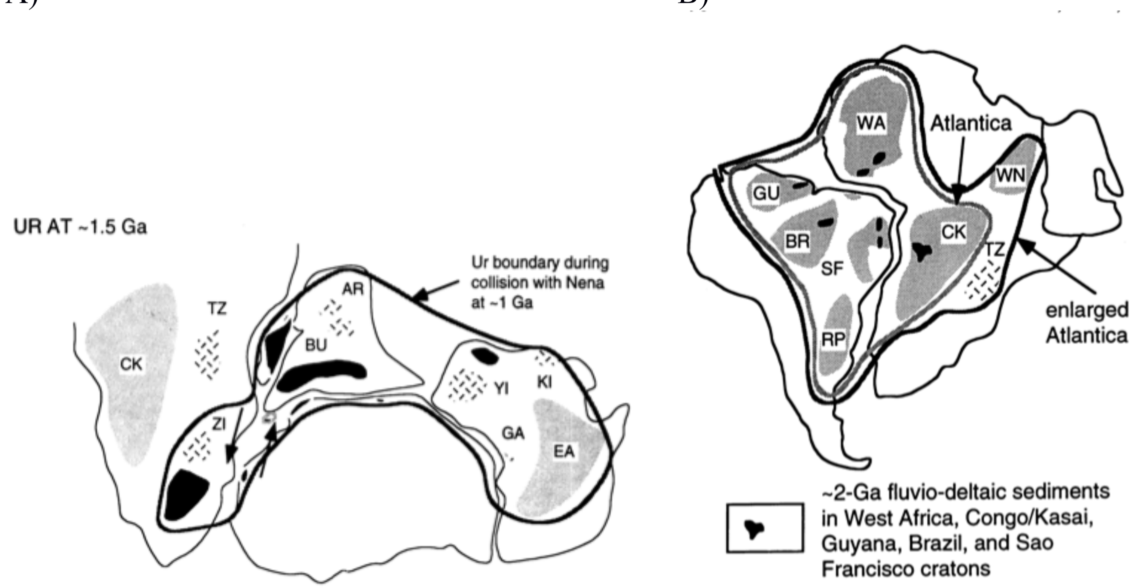

Figure 2: A) The continent of UR was originally composed of five cratons. These five are indicated by black enclosed regions; Kaapvaal Craton, Western Dharwar craton, Bhandara craton, Singhbhum craton, Pilbara craton. Other regions include Congo/ Kasai craton(CK), Tanzanian craton (TZ), Zimbabwe craton (ZI), Bundelkhand craton (BU), Aravalli craton (AR), Yilgarn craton (YI), Kimberley craton (KI), Gawler craton (GA),early Proterozoic areas in eastern Australia (EA). Arrows indicate possible sinistral

offset during consolidation of Gondwana B) Continent of Atlantica. Comprised of West African (WA), Congo/ Kasai(CK), Rio De Plata (RP), Guyana (GU), Brazil (BR), West Nile (WN), Tanzanian (TZ) and Sao Francisco (SF) cratons. Was enlarged by the addition of West Nile and Tanzanian cratons (Rogers, 1996).

Arctica is the second oldest continent assembled around 2500-1500 million years ago. It was comprised of North America, Greenland and Siberia. Between 1300-1600 million years ago Artica was enlarged through several different rifting and accretionary events. The first accretionary event occurred where Baltica joined the Baltic and Ukrainian shields. The next event occurred in the middle-Proterozoic where the North American terranes were added to the continent. The last event involved the collision of East Antarctica to Arctica. The several collisional events created a larger continent named Nena. During the Grenville event Nena joined with several other continents to form the supercontinent of Rodinia.

The last continent Atlanica, assembled around 2000 million years ago (Figure 2b). It is comprised of five cratons located on West Africa and eastern South America (shown by shaded areas in Figure 2b). Near 1.3 Ga the Tanzanian craton was accreted onto the eastern side of Atlantica during the early stages of the Kibaran event (hasher marks in Figure 2b).

Roughly 1000 million years ago Atlantica and Ur collided with Nena to form the continent of Rodinia during the Grenville event. Two major Grenville accretionary belts formed the continent. The primary collisional belt formed between the southeastern edge of Nena and the northwestern edge of Atlantica. The next belt formed between the western edge of NENA and eastern edge of the expanded continent of UR. The collision formed sutures between the Congo and Kaapvaal cratons. About 700 million years ago Rodinia broke apart into Ur, Siberia, Baltica, Laurentia, and Atlantica along two major rifts (refer to Appendix Figure A5). As time progressed the remaining blocks continued to fragment. Around 600 million years ago the remaining blocks began to reassemble. Gondwana assembled roughly 500 million years ago by the collision of Ur, Atlantica, eastern Antarctica, and the Arabian land mass. Nearly 200 million years later Gondwana, Laurentia, Baltica, Siberia together with masses that are present day parts of northern China and Kazakhstan combined to form Pangea (Figure 1).

About 300 million years ago the continent of Pangea began to fragment into smaller land masses. As the supercontinent continued to fragment, Africa remained joined to South America as it traversed southeastward while other continents Europe, North America, Australia and Antartica broke away from the supercontinent. Finally the African continent broke away from South American about 145 million years ago along a transect similar to the axis of the mid-Atlantic ridge that we see today and continued to propagate to its present day location. This brings Africa to it present day configuration where the Congo and West African cratons are located in the west and the Tanzanian, Zimbabwe and Kaapvaal cratons are located in the east with Oubanguides, Damara Ruwenzory, and Zambezi shear zones separating them (Figure 3).

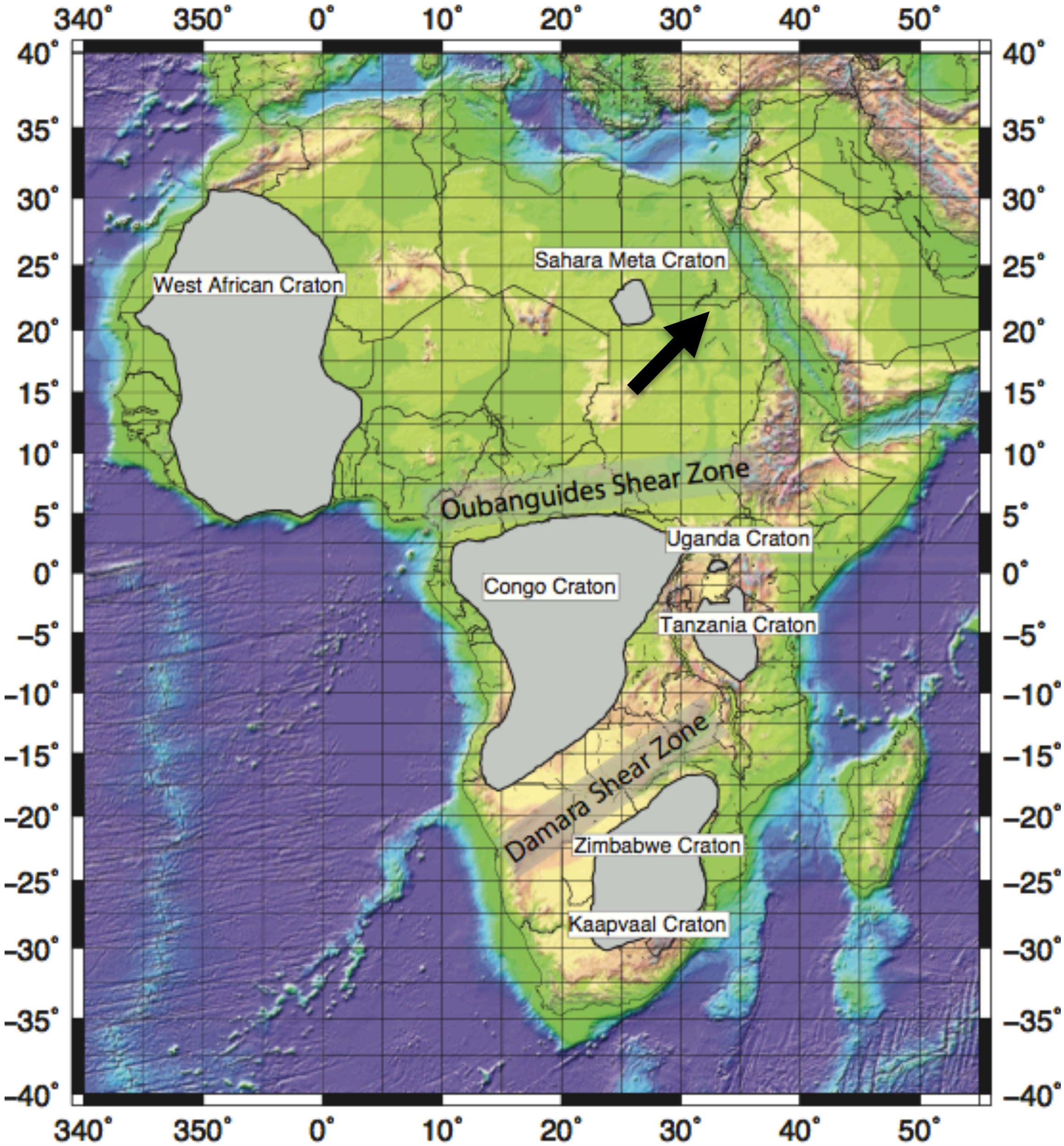

Figure 3: Displays the location of cratons and mobile belts on the African continent. The gray enclosed regions indicate craton locale. Large arrow indicates absolute plate motion (APM) of the African continent.

The African plate is a complex region, where a collective shear-wave splitting study has not been conducted. Although the tectonic history of the African continent is intricate and extensive, its history can provide in depth clues into possible inconsistencies that may be found throughout the continent. The African continent was once comprised of two separate landmasses but through many collisional and rifting events it finally assembled during the formation of the super continent Pangea. Its tectonic history of Africa, residing at the center of the Pangea land mass may be more complex than that of any other the continents. During the time of Pangea formation, all other continents were comprised of a singular cratonic land masses (Figure 1). The observation of six or more continental cratons on the African continent, suggests that this may be the result of a more complex evolutionary path.

1.2 Previous Studies of Stable Cratons

A surprisingly small number of measurements of seismic anisotropy have been made within the stable cratons of Africa. Analysis and modeling of SKS splitting was done within the Tanzania and Kenya region by Walker et al. (2004). Stations within the Tanzanian craton display fast directions that are fairly uniform at NW-SE with delay times of 0.3-0.8 s (refer to Appendix Figure 5). Two other studies have reported strong anisotropic velocities in the same NW-SE direction for Tanzanian craton stations including a study of Rayleigh waves which produce azimuthal anisotropy with an average direction of NNW-SSE and magnitude of 0.3% (Weeraratne et al., 2003) and individual SKS observations at nearby permanent GSN stations NAI and KMBO (Barroul and Ismail, 2001). Fossil anisotropy “frozen in” the cratonic lithosphere was suggested as a model for these observations by these authors. Although a comprehensive study was done by Silver et al. (2004) in the Kaapvaal craton, they found that nearly all stations in this array fell within shear zones surrounding the craton (refer to Appendix Figure A7). A few measurements in this study were made in the Zimbabwe craton which shows NE-SW fast directions with delay times of greater than 0.5 s. They found only one station within the Kaapvaal craton that has NW-SE azimuth. The seismic anisotropy magnitudes within continental cratons in Africa are generally small with shear wave splitting delay times ≤ to 0.5 s. These studies also indicate that anisotropic fabric is prevalent in cratons but is not consistent between cratonic regions. This suggests that these observations may represent fossil anisotropy frozen into the lithosphere during previous tectonic events.

1.3 Previous Studies of Rift Zones

Seismic anisotropy in rift zones of the African continent display the largest shear wave splitting delay times and the strongest anisotropic fabric. The direction of anisotropy, however, is highly variable. If we consider these results in the broader context of African continental cratons surrounded by shear zones, these observations seem to follow a pattern of rift parallel orientation. This likely occurs due to high shear stresses produced between stable cratons during tectonic accretion events and collisions. Fast directions in the region of the Main Ethiopian rift are NNE-SSW with delay times ranging from 0.5 s-1.7 s (Gashawbeza et al., 2004; refer to Appendix Figure A8). In a study done in the Eastern Branch of the East African Rift splitting directions are parallel to the strike of the rift axis (Gao et al., 1997; refer to Appendix Figure A9). Walker et al. (2004) show that fast directions for stations surrounding the Tanzanian craton appear to wrap around the craton border (refer to Appendix Figure A10). Splitting times outside the craton are larger and range from 1.0-1.5 s. Silver et al. (2004) determined seismic anisotropy within In the Kaapvaal region of southern Africa shear wave splitting measurements are dominantly NE-SW on the western border of the Kaapvaal craton. The trend of splitting fast measurements rotate to E-W near the Limpopo belt shear zone which marks the collision zone between the Kaapvaal and Zimbabwe shields. All splitting directions in Kaapvaal project were less than 0.5 s. The majority of measurements which occur within the shear zones surrounding the Kaapvaal craton are consistent with the axis of shear. With only a few exceptions, seismic anisotropy within continental cratons have smaller magnitudes (with shear wave splitting delay times ≤ 0.5 s) than anisotropy observed in shear zones (where shear wave splitting delay times ranging from 1.0-2.5 s). When fast directions for shear zones occur on a NE-SW azimuth, there is ambiguity between two possible sources including alignment with the axis shear or alignment with the APM direction for Africa which is moving 50° to the NE (DeMets et al., 1994).

Chapter 2 Methodology

2.1 Data Used in This Study

The data collected for this study consists of SKS, SKKS, SKIKS, PSKS, and SSKS phases that lie within a distance range of 80°-130° (Figure 4). The distribution of earthquakes in this study is fairly evenly distributed although events are subsequently missing from the NW and S quadrants (Figure 4). Evenly distributed events are necessary for testing the consistency of anisotropic values. However a single station generally only produces one or two measurements in the results presented within this paper. Thus the azimuthal distribution shown represents the entire study rather than a complete distribution at each station. The data was primarily collected from the Africa Array network and the Global Seismic Network (GSN) (refer to Appendix Figure A11). I have used 28 different earthquake events that occur deeper than 10 km and are greater than Mb 5.0.

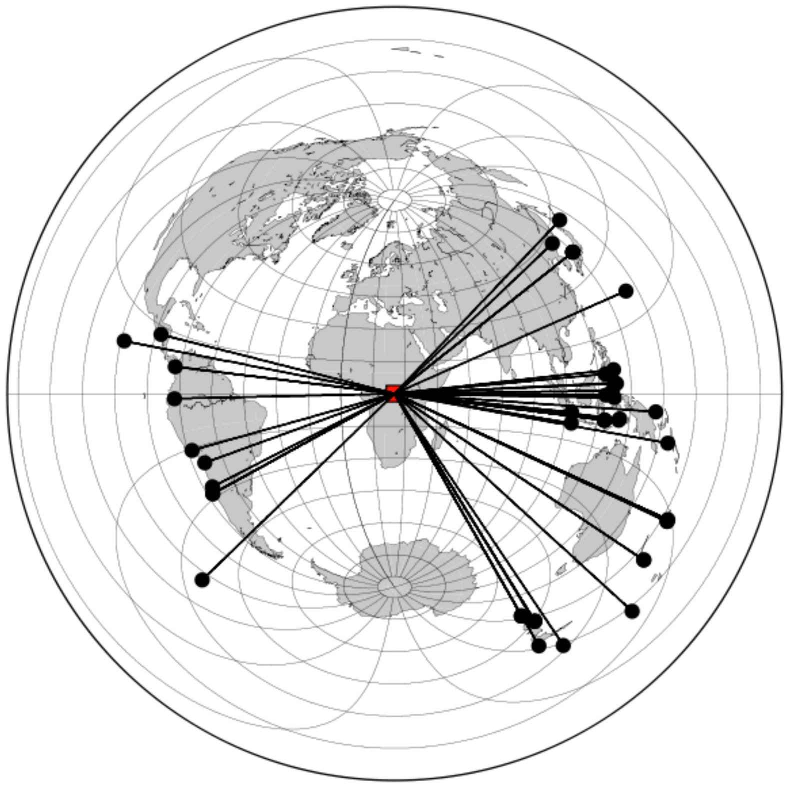

Figure 4: Distribution of earthquakes within this study. Enclosed circles represent event locations while lines indicate ray paths. Ray paths are linear when plotted on an equidistant map. Ray paths are polar projections in which all distances measured from the center of the map along any longitudinal line are accurate.

I have used events that display the presence of SKS phases such as: SKS, SKKS, PSKS, SSKS, SKIKS. These phases are particularly beneficial because they only record the anisotropy present in the mantle on the receiver side (refer to Appendix Figure A12). Generally only P-waves can propagate through the core. Consequently a S-wave propagating throughout the mantle is converted to a P-wave (K phase) upon entry into the outer core, it is then converted back to an S-wave upon its departure. Any anisotropy that is recorded by the S-wave on the source side is eliminated. The anisotropy present in the mantle on receiver side will produce energy on the transverse component.

2.2 Methodology

Anisotropy can be described as the variation of velocity that is given as a function of both propagation and polarization direction of seismic waves. There are two types of anisotropy, propagation and polarization anisotropy. The comparison of the values from two seismic waves traveling on different paths through the same medium is called propagation anisotropy. This is also commonly referred to as azimuthal anisotropy. Polarization anisotropy can be simply defined to occur in a material with lattice-preferred orientation where the seismic waves will travel faster in the direction of alignment. As the shear wave passes through the anisotropic medium the first horizontal component becomes separated from the second horizontal component.

Here, we calculate polarization anisotropy from SKS waves recorded by Africa Array and GSN seismic stations deployed throughout the African continent. We use the graphical user interface program Splitlab for our analysis (Wustefeld et al., 2007). This program allows for use of different theoretical methods to measure anisotropy including rotation correlation, minimum energy, and minimizing the smallest eigenvalue (λ_2). In this study we use the method that minimizes λ_2 following Silver and Chan [1991]. In our analysis, we search for the SKS phase which produces signal to noise ratios greater than three on the transverse component. A grid-search is performed to find the fast axis (f) and the delay time (dt) that minimizes λ_2 and will best remove the observed splitting.

2. 3 Splitting Analysis

The SKS analysis technique is displayed in Figure 5. All seismograms in this study are filtered with a bandpass filter of 0.01 Hz-0.5 Hz. A window is selected around the SKS phase (gray shaded area in Figure 5a) that best displays good signal to noise ratio that is 3 or greater. Figure 5b demonstrates the correlation between the corrected fast and slow components after the resolved splitting is removed. The highest quality result should remove splitting completely and will show high correlation between the solid and dashes lines. Particle motion can be described by the energy on the two horizontals and will be non-linear if the shear wave is split, but should become linear once splitting has been removed as shown in figure 5c. The 95% confidence limit for the fast direction and delay time is plotted in the gray shaded bold contour in figure 5d. The results for the selected window (Figure 5e) for an event recorded at TEZI on the 24th of June 2006 are displayed in figures 5f-h.

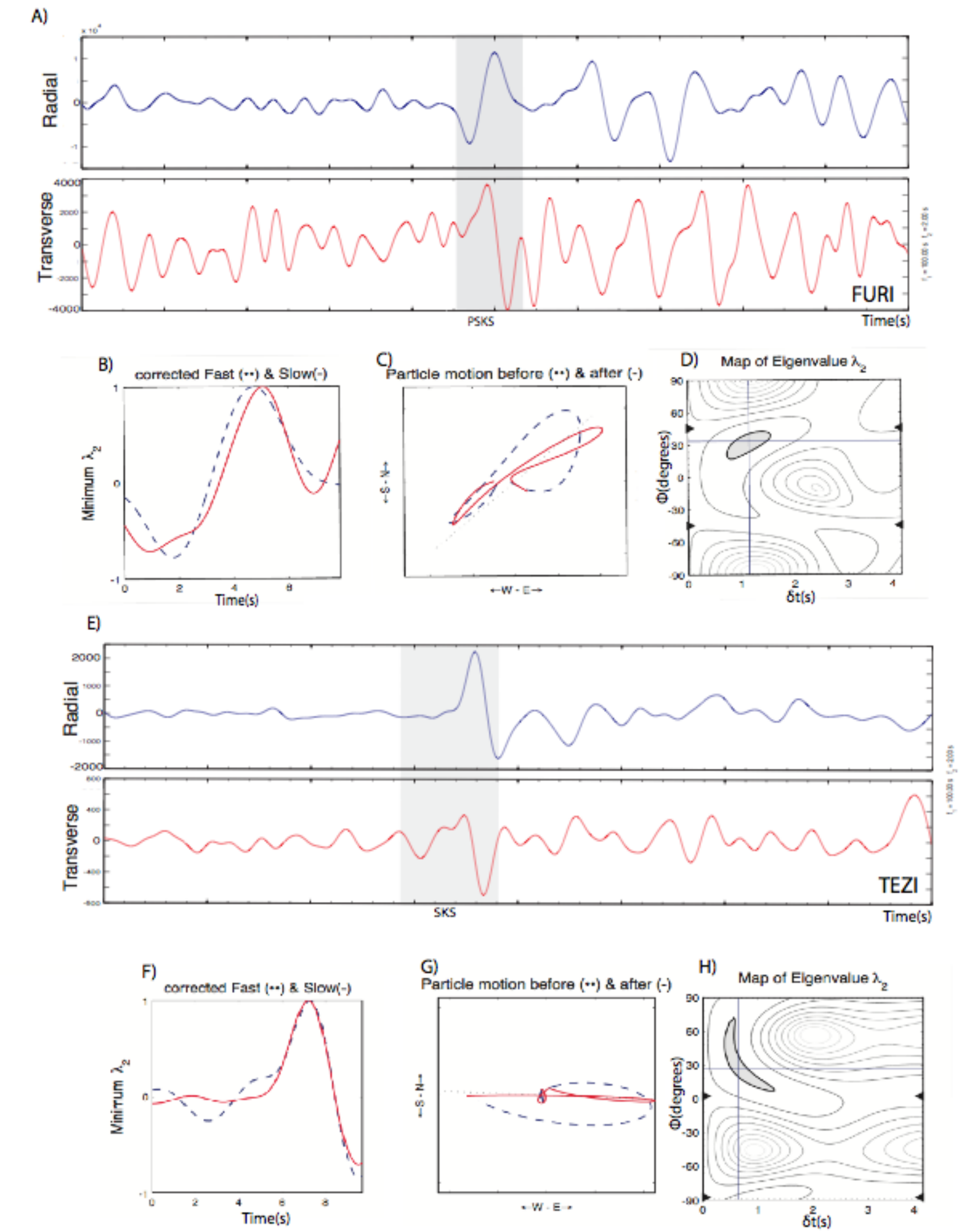

Figure 5: SKS analysis technique. Top record (blue) is the radial component and second record (red) is the transverse component. Gray shaded area indicates window used in

shear wave splitting analysis. The corrected fast and slow components minimizing l_2 are shown in the lower left. The linearity of particle motion before and after corrections is displayed in the lowermost middle panel. The final solution for the fast direction and delay time is displayed in the lower right. The 95% confidence limit is shown by a dark shaded contour.

In this analysis, I have classified the quality of each measurement based on 5 criteria; the phase clarity and signal to noise ratio on the horizontal components, clarity of the phase on the transverse component, the correlation between the fast and slow components, the linearity before and after correction is applied, and the correlation between three different methods. For quality purposes we first obtain a preliminary assessment of anisotropy by using three different methods; rotation correlation method, Silver and Chan minimizing λ_2 method, Silver and Chan ratio of λ_1/λ_2. I have given rates for each measurement on a scale of excellent, good, fair. Where excellent has a total point value ranging from 25-20 (where each of the criteria mentioned above has a maximum possibility of 5 points) of the required criteria and a good result has a value ranging from 19-14, fair quality ranges from 13-8 and poor ranges from 7-0. Although the two events presented in figure 5 appear to have similar signal to noise ratio, the event recorded at TEZI (Figure 5e) has a nearly 7 times larger magnitude than the event recorded at FURI and has higher signal to noise ratio with greater clarity. The event recorded at TEZI produces results that can be classified as higher quality than the event recorded at FURI. The corrected fast and slow components in figure 5f are better correlated than those in figure 5b. When splitting is removed in both events, particle motion is more linear in figure 5g than figure 5c. The 95% confidence limit is not as concentric in figure 5h as figure 5d. The quality assessment of each splitting result is listed in Table 1.

Date	Q	lat	lon	Phase	Mb	station	BAZ	φ	φ error	δt	δt error
19950205	E	-37.71	178.8	SKKS	7.1	NAI	142.1	-22	0	1.6	0
19990403	G	13.17	-87.63	sSKS	6.0	KOWA	281.3	-49	6	0.9	0.15
20031229	E	42.40	144.6	pSKS	6.1	FURI	45.5	33	10.5	1.2	0.4
20050205	E	5.29	123.3	SKS	7.1	LBTB	88.44	-12	34	0.4	0.6
20050302	E	-6.53	129.9	SKIKS	7.1	LBTB	102.1	-32	41	1.2	1
20050411	E	8.66	-104	SKS	5.5	TSUM	268.2	-24	27	1.2	0.2
20050613	G	-19.99	-69.20	SKS	7.8	PKA	251.6	16	9	0.7	0.05
20050908	E	0.77	126.3	sSKS	5.7	KMBO	89.21	61	9	1.1	0.1
20060102	E	-19.88	-178	PKS	7.2	LBTB	150.5	-35	51	0.4	0.4
20060123	G	6.84	-77.80	pSKS	6.1	KTWE	273.3	-11	22.5	0.6	0.5
20060123	G	6.84	-77.80	SKS	6.1	TEZI	273	-75	15	0.6	0.05
20060430	G	-26.99	-70.80	SKKS	6.6	BFT	241.2	29	14.5	0.9	0.45
20060516	E	-31.56	-179	SKIKS	7.4	SWZ	156.6	-43	59	0.4	0.6
20060624	E	-0.43	123.2	SKS	6.3	KTWE	91.5	-4	2	1.7	0.2
20060624	E	-0.43	123.2	SKS	6.3	TEZI	92.36	26	25.5	0.6	0.35
20060624	E	-0.43	123.2	SKS	6.3	SWZ	94	8	9	0.8	0.25
20060716	G	-28.60	-72.39	sSKS	6.2	MZM	238.3	-42	4.5	2.5	0.1
20060716	E	-28.60	-72.39	SKKS	6.2	TEZI	240.2	46	31.5	0.8	0.65
20060716	G	-28.60	-72.39	pSKS	6.2	ZOMB	237.5	-5	16	1.4	0.6
20060716	G	-28.60	-72.39	SKKS	6.2	CNG	238.1	74	33	1.6	0.3
20060807	E	-15.87	167.8	SKKS	6.8	GRM	136.7	-29	47	1.4	1.3
20060807	E	-15.87	167.7	sSKS	6.8	HVD	136.6	-13	7	0.6	0.1
20060930	E	-15.51	-72.99	SKKS	5.9	MSKU	254.6	17	20	0.8	0.2
20061129	E	2.55	128.3	SKKS	6.2	DESE	87.8	56	13.5	1.5	0.2
20070220	E	-1.06	127.1	pSKS	6.7	HVD	96.9	-77	9	1.3	0.4
20070413	E	-35.00	-108.8	SKS	6.1	MBAR	223.2	5	24	1.7	0.2
20070607	G	-3.38	146.8	SKIKS	6.2	AAUS	90.59	-17	22	2.1	0.2
20070628	G	-7.95	154.6	SKS	6.7	AAUS	94.41	18	11	1.9	0.25
20070630	E	21.10	144.8	sSKS	6.6	EKNA	58	-32	25.5	0.7	0.45
20070716	G	36.79	134.9	SKS	6.8	PKA	63.43	75	26	0.9	0.8
20070716	G	36.79	134.9	SKS	6.8	GRM	64.52	13	18	0.8	0.4
20070716	E	36.79	134.9	SKS	6.8	CVNA	65.32	-25	65	0.6	0.9
20070716	E	36.79	134.9	SKS	6.8	MOPA	58.64	35	45	0.6	0.7
20070726	E	2.8	127.5	SKS	6.9	MOPA	89.86	48	23	1.1	0.9
20070801	G	-15.67	167.6	SKS	7.2	CNG	128.9	-11	25	1.3	0.4
20070801	E	-15.70	167.6	SKIKS	7.2	MOPA	128.2	30	46.5	0.9	0.7
20070808	E	-5.97	107.7	SKKS	7.5	SWZ	91.85	12	42	0.9	0.5
20070820	E	6.16	127.4	pSKS	6.4	MOPA	86.7	35	1	1.2	0.05
20070928	G	-21.44	169.4	SKKS	6.3	HVD	141.8	-78	3	1.3	0.05
20070930	E	-49.41	163.3	sSKS	6.6	GRM	153.5	-81	7	1.8	0.3
20070930	G	-49.41	163.3	SKKIKS	6.6	HVD	154.1	40	32.5	2.3	0.2
20071015	G	-44.70	167.5	sSKS	6.8	HVD	153.8	56	18.5	1.3	0.25
20071015	E	-44.70	167.5	SKKS	6.1	LSZ	150.6	73	11	1.4	0.15
20071015	G	-44.70	167.5	pSKS	6.1	LSZ	150.6	81	32	1.1	0.15
20071015	G	-44.70	167.5	psks	6.8	CVNA	157.4	23	18	1.3	0.3
20071015	E	-44.70	167.5	sks	6.8	CVNA	157.4	-1	18	1.2	0.35
20091024	E	-6.16	130.4	SKS	6.9	GRM	102.8	67	45	0.5	0.4
20090828	E	-7.12	123.4	SKS	6.9	GRM	99.72	82	53	0.6	0.8
20090828	E	-7.12	123.4	SKS	6.9	CVNA	57.38	-75	4	1.1	0.3
20090828	E	-7.12	123.4	SKKS	6.9	GRM	99.72	64	58	1.2	0.6
20090828	E	-7.12	123.4	SKS	6.9	SWZ	100.1	14	10	1.1	0.8
20100218	G	42.58	130.5	SKKS	6.9	CVNA	103.3	21	26	0.8	0.4
20100712	E	-1.26	-77.3	pSKS	7.1	PKA	263.9	50	25	0.8	0.6
20090809	G	33.14	138	SKS	7.1	LBTB	65.0	63	18	0.9	0.8
20070716	G	36.79	134.9	SKKS	6.8	LBTB	60.3	60	43	1.2	1.0

Table 1: Shows results for study region. Displays date of event, quality of measurement (Q), latitude, longitude, phase, magnitude (Mb), station name, Backazimuth (BAZ), fast direction (ϕ) along with error and delay time (δt) along with its error. The splitting quality (Q) is rated from P-G-E for Poor, Good, and Excellent. Only results for Good and Excellent are shown here.

Chapter 3 Shear Wave Splitting Results

Below, I will describe my splitting results as shown in figure 6 for stations in North Africa moving progressively to the southern most region. The splitting measurements listed in Table 1 are displayed on the map below in figure 6. Showing the fast direction with respect to north. The length of each bar is scaled to the splitting delay time (δt) as indicated by the scale bar in the lower left.

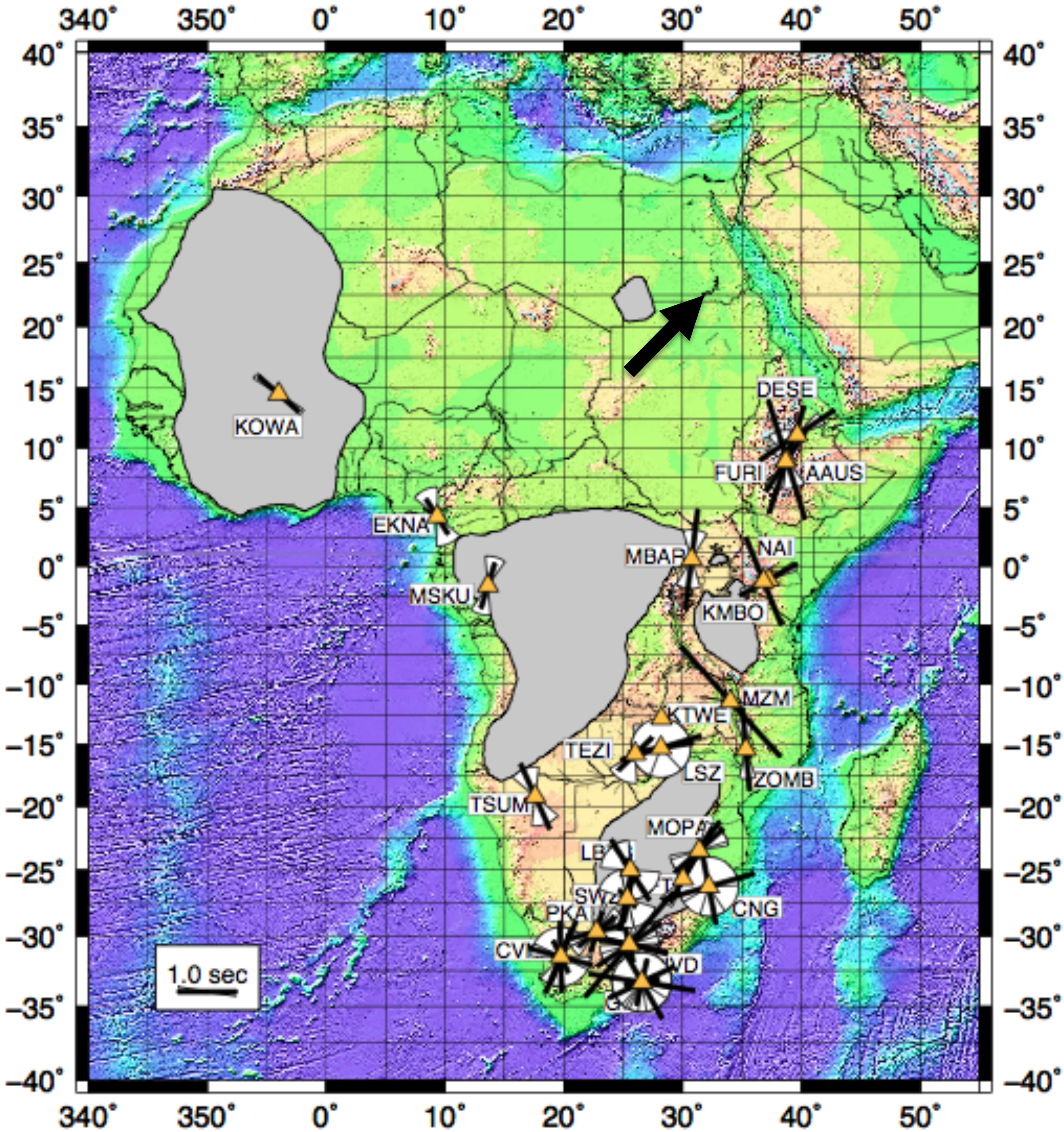

Figure 6: Splitting directions with corresponding error bars. Solid lines show the splitting direction with their length corresponding to the length of delay time. Triangles represent station location. White enclosed regions displays the range in error for each result. Gray regions indicate locale of cratons throughout the continent. Solid black arrow indicates APM.

3.1 North Africa Stations

The most northern stations is KOWA, which is the only station in our study located in the west African craton. The splitting measurement at KOWA displays a NW-SE fast direction and a delay time of 0.9 s. Stations located in northeast Africa (DESE, FURI, AAUS) primarily all have fast directions of NE-SW with splitting times between 1.2 s and 2.1 s. Although the splitting direction may differ between theses stations they display an average fast direction of 37^{o} E of N +/- 35^{o}.as shown by the white triangles below the splitting bar. One station, EKNA, located in the Cameroon region, at the western coastal edge of the central African shear zone, produces a NW-SE fast direction and fairly small delay time of 0.7 s. Discussions below identify this fast direction to be oriented perpendicular to the shear zone axis.

3.2 Central Africa Stations

In the region of Tanzania, stations NAI, KMBO, MBAR, MZM, and ZOMB display delay times range from 0.9 s-2.0 s. The delay times of the three stations located near the upper portion of the craton (NAI, KMBO, and MBAR) have delay times that are within relative error of one another. NAI gives a delay time 1.6 s while MBAR has a similar delay time of 1.7 s. KMBO has a smaller delay time of 1.1 s. MZM and ZOMB lie along the lower perimeter of the Tanzanian craton have delay times that vary from what to what 1.4-2.5 s. The fast directions in this region vary widely throughout. MBAR and KMBO both have fast directions of NE-SW. While NAI, MZM, and ZOMB have fast directions of NW-SE. MSKU and TSUM lie on opposing ends of the Congo craton. MSKU has a fast direction of NE-SW with a delay time of 0.8 s. While TSUM has a fast direction of NW-SE with a delay time of 1.2s. TEZI, LSZ, are located in central Africa, skirt the Congo craton and display consistent NNE fast directions and delay times ranging from 0.6-1.7 s. KTWE has splitting direction of NNW and an average delay time of 1.15s. Two stations, LSZ and TEZI, located in the Damara suture belt between the Congo and Kaapvaal cratons, display a NE-SW fast direction parallel to the suture axis. LSZ has an average delay time of 1.25 s while TEZI has an average delay time of 0.6 s.

3.3 South Africa Stations

In the Kaapvaal craton region of southern Africa, the average anisotropic direction is NNE with a delay time ranging from 0.4 to 1.7 s. Stations CVNA, PKA and HVD in the southern tip of Africa, south of the Kaapvaal craton, reveal a NE, NW and E-W fast directions with delay times that vary from 0.5 to 1.3 s. Several splitting measurements are made for the southern station HVD which have event back azimuths that vary (see Figure 4) producing NW-SE fast directions that are variable and range from NW-SW to WNW. GRM is located in the southeastern region of Africa and obtains a fast directions that are E-W, NNE and NW-SE similar to results recorded at HVD. Its delay time fall between 0.5 to 1.8 s.

3.4 Back Azimuthal Dependence of Seismic Anisotropy

Numerous stations throughout our study yield varying splitting directions. We attempt to explain this inconsistency by plotting results observed at each station on a rose diagram (Figure 7). Rose diagrams simultaneously display the back-azimuth of the event, fast direction and ray parameter of each earthquakes ray path (refer to Appendix Figure A12). It also displays the arrival azimuth in map view and plots it on a circular diagram 0°-360°. The ray parameter describes the incidence angle of the ray path where the value of p ranges from 2°-8° (refer to appendix Figure A13).

The rose diagrams for each station shown in figure 7 are organized by geographic location from north to south as observed in the map of figure 6. Most of the stations in northern Africa either have a single measurement or have splits, which are consistent with each other. TEZI is located in the Damara suture belt in central Africa south of the Congo craton and has produced three results with different splitting directions. Two of the directions are sub-parallel to the APM while the other is E-W. This difference in direction can be attributed to the varying back-azimuths of the earthquake raypaths. The two events with similar fast directions of NE come from the east and SW direction region. The event coming from the west shows a smaller delay time than the others with an EW fast direction suggesting that there may be a boundary in structure between the two western events at roughly WSW where anisotropy is NE-SW east of this boundary and anisotropy is E-W west of this boundary. This structural boundary may be the division between the Congo craton edge and the Damara shear zone. It is possible that the western event samples the edge of the Congo craton and indicates fossil cratonic fabric. The small delay times of this measurement strengthens this argument as it is consistent with the small delay times observed for most cratonic regions in Africa, while the other event comes from the eastern region.

The next station that yields varying splitting results is CNG, which is located east of the Kaapvaal craton. The event which arrives from a SW azimuth yields a NE-SW splitting direction but the event which arrives from the SE azimuth displays a NNW fast azimuth. We note that the event from the SW azimuth may sample mantle structure of other stations which lie to the west of CNG such as BFT, SWZ, LBTB and

MOPA which both display fast directions consistent with the value at NE-SW. The event which arrives from the SE may sample different mantle structure including oceanic mantle as CNG is located near the continent/ocean eastern boundary.

The last station displaying inconsistent results is HVD that is located in the southern most tip of Africa. It produces five splitting values with two different splitting directions. The splitting directions that are display a NE-SW fast direction have similar back-azimuth arrivals from the SSE. Two results show splitting directions that have a NW-SE fast direction, which are produced by events arriving from the ESE or SE. We suggest that these 2 groups of observations may sample different distinctive material structure. Note that the stations to the west of HVD all produce fast directions of NE-SW which is consistent with the two event arriving from a SSE back azimuth and may sample similar structure. The observation from station GRM located to the east of HVD, produces a NW-SE azimuth that is consistent with events at HVD arriving from the SE suggesting they sample similar structure. This indicates a tight lateral constraint of a structural boundary that may exist along a SE-NW azimuth from HVD where events and structure east of this boundary display SW-NE fast directions and events and structure west of this boundary display NW-SE fast directions.

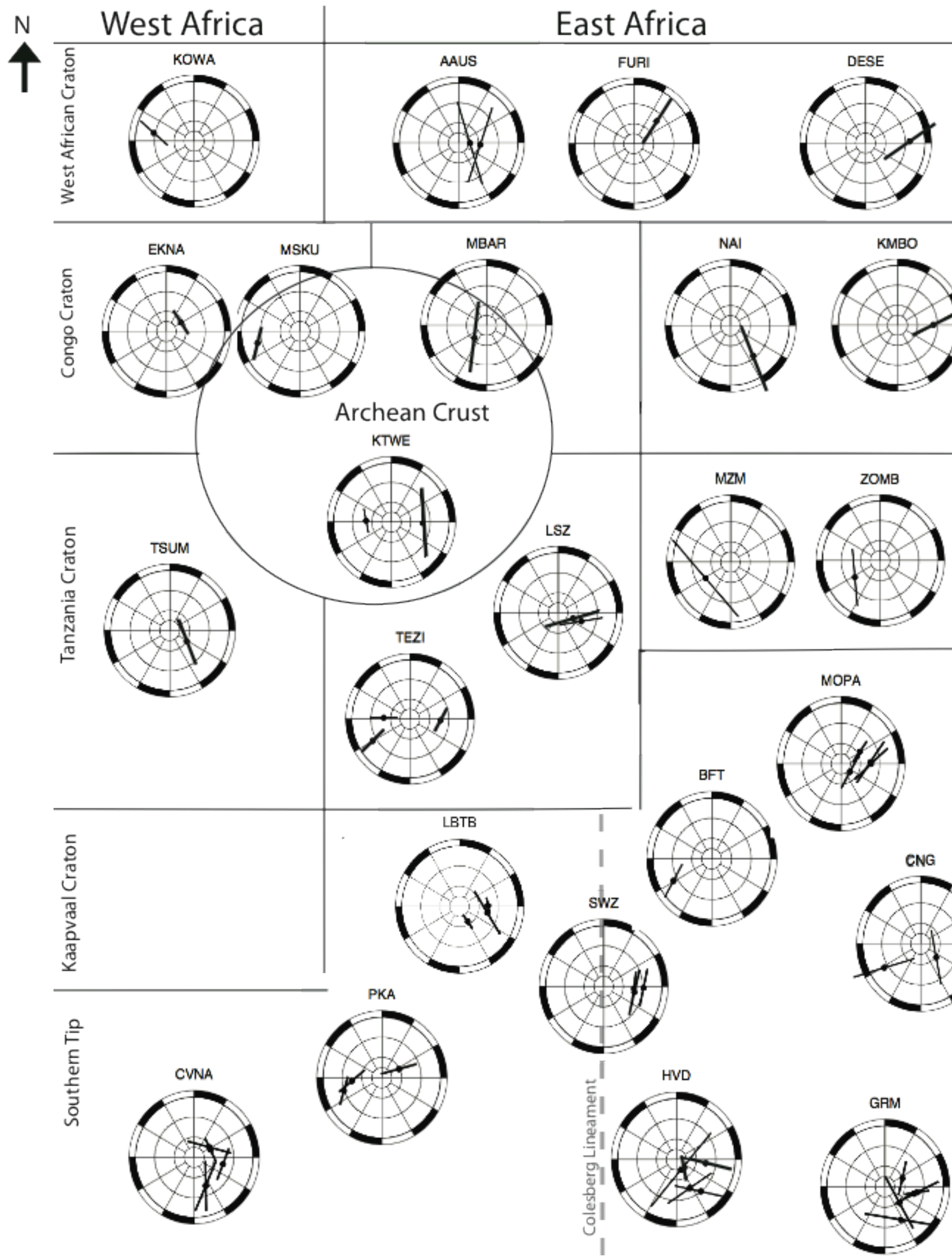

Figure 7: Rose diagrams for each station based on station location on continent. Solid line indicates splitting fats direction. Position of splitting result on the diagram indicates back-azimuth of the event and ray parameter. Back azimuth is plotted on each circular diagram from 0° to 360°(clockwise). Ray parameter is plotted on gray circular lines starting with central point with a value of two Ray parameter begins with the center increase by intervals of two.

Chapter 4 Discussion

4.1 Stable Cratons

4.1.1 Continental Cratons in North Africa

KOWA is located in the West African craton and displays a fast direction of NW-SE and is not consistent with APM. We suggest that this result can be categorized as remnant fabric frozen into the lithosphere of the West African craton during previous events. The map of tectonic collision of Pangea is shown in figure 2, shows the collisional zone between North America and northwest Africa around 300 Ma. The next and most recent rifting event separated Africa from North America along a rift zone that is parallel to the collision zone. Thus the direction of rifting is parallel to the fast direction displayed by KOWA.

In the vicinity of the Congo craton, MSKU and TSUM are the two stations that sample this region (Figure 6). Although MSKU exhibits a fast direction that is 17 degrees E of N, within error, this may rotate to an azimuth that is NNW. The observations at our western most stations (KOWA, EKNA, MSKU, and TSUM) may thus display a consistent azimuth in the NNW direction. We suggest that these stations may indicate anisotropic fabric that is “frozen in” to the lithosphere from a previous tectonic event. The Congo and West African craton were once a part of the land mass Atlantica as shown in figure 1B, which also includes cratons observed today in South America. The consistency in observations between all of our stations along the western border of Africa may imply that Atlantica as a whole may have anisotropic fabric that is oriented in the NW-SE direction. The Tanzanian craton is also a member of the Atlantica land mass with a similar NW-SE fast direction within the craton interior as observed from both SKS (Barroul and Ismail 2001; Walker et al., 2004) and surface waves studies (Weeraratne et al., 2003). Splitting observations at stations MBAR and KTWE although located within shear zones today, are part of surface outcrops that are identified as Archean crust by previous studies (Figure 8). The fast direction for these stations may also be oriented in the NNW direction taken within error. (Note LSZ and two observations from TEZI which have NNE fast directions have a back azimuth origin from the east which samples a different tectonic region, and does not conflict with this interpretation). The consistent direction of anisotropy in the NW-SW azimuth observed by all our stations located on cratons in northern Africa as well as consistency with previous studies in this region suggest that an axis of NW-SE anisotropic fabric is widespread in cratonic lithosphere over a large part of north Africa. The boundary of this northern cratonic region might be consistent with the major suture zone shown in figure 2 when the Zimbabwe and Kaapvaal cratons accreted onto Africa at the base of the Congo craton. Improved seismic coverage within the continental cratons of West Africa and the Congo would further test this result. Additionally, seismic studies of the Guyana, Brazillian, and Sao Francisco cratons in South America might resolve whether this uniform fabric is continuous within other cratonic lithosphere of Atlantica.

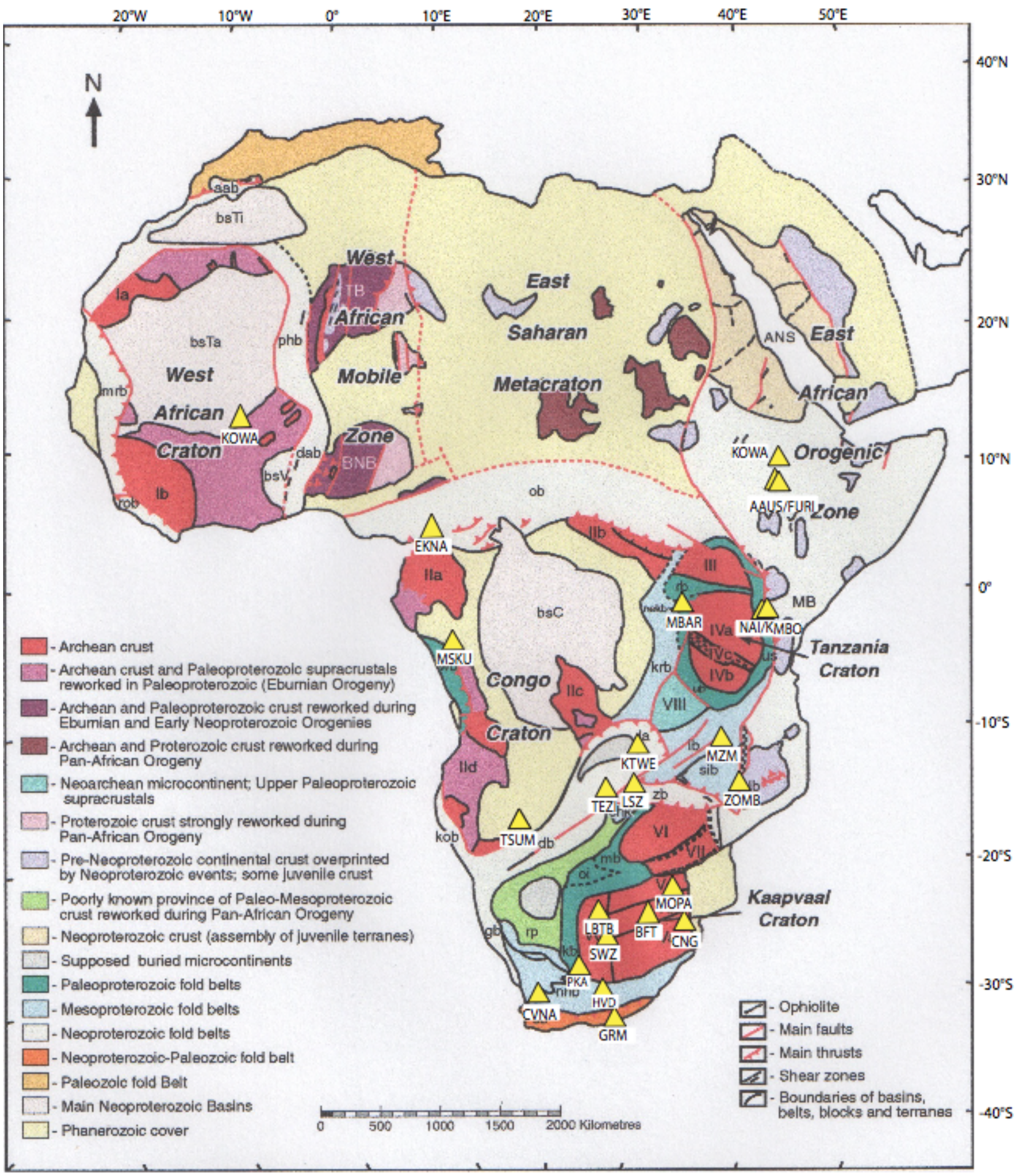

Figure 8: Displays station location in relation to geological units on the continent. Blue triangles are station location. Cratons and Micro- continents: West African Craton (Ia—Reguibat Shield; Ib—Man-Lèo Shield); Congo Craton (IIa—Gabon-Kamerun Shield; IIb—Bomu- Kibalian Shield; IIc—Kasai Shield; IId—Angolan Shield); Ugandan Craton—III; Tanzanian Craton (IVa—Northern Terrane; IVb— Southern Terrane; IVc—Dodoma Zone); Kaapvaal Craton (Va—Southern Terrane; Vb—Central Terrane; Vc—Pietersburg Terrane; Vd—Western Terrane); Zimbabwe Craton—VI; Limpopo Block—

VII; Bangweleu Block—VIII. West African Mobile Zone: TB—Tuareg Block; BNB—Benin-Nigerian Block. East African Orogenic Zone: ANS—Arabian-Nubian Shield; MB—Mozambique Orogenic Belt. Fold Belts: Paleoproterozoic Belts: ub—Ubendian; us—Usagaran; rb—Ruwenzory; kb—Kheis; oi—Okwa inlier; mb—Magondi; wb—West Central African; nekb—North-Eastern Kibaran. Paleo-Mesoproterozoic Province: rp—Rehoboth. Mesoproterozoic Belts: krb—Kibaran; ib—Irumide; sib—Southern Irumide; chk—Chomo-Kolomo; nnb—Namaqua-Natal. Neoproterozoic Belts: zb—Zambezi; la—Lufilian arc; db—Damara; kob—Kaoko; gb—Gariep; ob—Oubanguides; aab—Anti-Atlas; phb—Pharusian; dab—Dahomeyean; rob—Rockellides; mrb—Mauritanides; lb—Lurio; sb—Saldania. Neoproterozoic Basins: bsC—Congo; bsTa—Taoudeni; bsTi—Tindouf; bsV—Volta (adapted after Begg et al., 2009).

4.1.2 Kaapvaal Craton

We have only one station in our study, which samples the Kaapvaal craton interior. CNG is positioned on the edge of the craton. It has two measurements arriving from different backazimuths. The event from the SW samples the Kaapvaal craton and indicates a NE-SW fast direction which is sub-parallel to the APM as well as the shear zones identified by previous studies of the Kaapvaal craton (Silver et al., 2004). Note that if this single event samples the cratonic lithosphere the NE-SW direction is different from the remnant lithospheric fabric suggested above for all cratons in northern Africa. The other measurement at CNG arrives from a SE back azimuth and is perpendicular to the APM with a NNW fast direction. This event likely samples coastal or even marine mantle structure due to the proximity of CNG to the coastline. The SW Indian ridge spreading center located off the eastern shore of south Africa (see Figure 8) is an example of oblique spreading where the spreading direction is not perpendicular to the spreading ridge axis. The spreading direction can be observed by the orientation of transform faults on the seafloor which are oriented roughly N-S.

It can be clearly seen from the presented results that anisotropy in cratons are not consistent with APM of the African plate today. We suggest these old structures with

Archean ages that span nearly half of the Earth's history represent fossil anisotropy from previous tectonic events during craton formation. The West African, Congo, and Tanzanian cratons each maintain fast directions of NW-SE while the Zimbabwe and Kaapvaal cratons maintain directions of NNE NE-SW. We note that the major division on the continent between splitting directions can be attributed to the boundary of the collision between the UR and Atlantica during the assembly of the super continent of Pangea (Figure 2) across the Damara shear zone. The anisotropic fabric preserved in Africa cratonic lithosphere today may give us clues as to the tectonic behavior of large continental land masses active billions of years ago.

4.2 Rift Zones

4.2.1 The Main Ethiopian Rift System

Near the eastern most part of the East African rift system, stations located in the main Ethiopian rift present fast directions sub-parallel to the APM and to the rifts axis (DESE,AAUS, and FURI). These stations have fast directions that are within narrow error of one another and delay times that range from 1.2-2.1 s. We also consider KMBO in this group although located far south of these stations. This station has a delay time of 1.1 s. The event observed at this station has a NE back azimuth which produces a similar NE-SW fast direction, indicating this fabric may extend as far south as 5° North or even the equator. All of these stations have events that originate from the back azimuths that range from NE to west consequently displaying that the mantle anisotropic structure in this part of the East African rift has a fairly uniform NE-SW orientation aligned with the rift axis.

4.2.2 The Eastern and Western Branch of the East African Rift.

Stations situated within close proximity to the Tazania craton (NAI, KMBO, MZM, MBAR) display fast directions that are contoured around the craton perimeter within the axis of the Eastern and Western Branch of the East African rift. Many of the stations located NE of the Tanzanian craton yield fast directions that are NNE and NNW . Station NAI yields a NNW splitting direction and a delay time of 1.6 s. Stations MZM and ZOMB both have a fast directions of NW-SE that are consistent with rifting around the perimeter of the Tanzanian craton. These stations have delay times ranging from 1.4-2.5 s. ZOMB is located further south along the Malawi rift that extends south of Tanzania, thus the NNW fast direction may reflect alignment with the rift axis. All of the stations surrounding the Tanzanian rift system have fast directions that mimic rift axis of the Eastern and Western Rift branches of the East African rift. This result is consistent with previous shear wave splitting studies with stations located in the rift zones (Walker et al., 2004, Barruol and Ismail 2001).

Stations KTWE, LSZ, and TEZI are located southwest of the Tanzanian craton and have delay times that range from 0.6-1.7 s. KTWE lies in Archean crust and has a splitting direction of NNW. Stations TEZI, and LSZ lie in the Damara rift zone between the Congo and Kaapvaal cratons and have fast directions that are parallel to the shear axis (Figure 8). This direction is also roughly parallel to the APM of Africa today. Although KTWE, LSZ and TEZI are within close proximity to one another they maintain varying splitting directions. This inconsistency can be attributed to the different units that each station samples (Figure 8).

4.2.3 Kaapvaal Craton

There are six stations that surround the boundary of the Kaapvaal craton (Figure 9). Station SWZ is located near the Colesberg lineament within the Ventersdorp magmatic rift system. The dominant NNE splitting direction of all fast directions from SWZ are consistent with results produced by Silver et al. (2004) in this region and are nearly parallel to the N-S collisional zone between the eastern Kaapvaal craton (Witswatersrand Block) and the Kimberley block along the Colesberg lineament. LBTB is located north of the Ventersdorp region at the junction of the Colesberg and E-W trending Thabazimbi–Murchison lineaments and produces fast directions rotate NE-SW at this junction and produce delay times between 0.4-1.2 s. This is consistent with observations made by Silver et al. (2004) at the collisional belt between the northern accreting Pietersburg block and the eastern Kaapvaal craton. Station BFT is located in the eastern Kaapvaal craton and produces a NE-SW fast direction. PKA is located at the southwestern boundary of the Kaapvaal shield in the Kimberley block. It produces fast directions of NNE from western-back azimuths that rotate to the ENE from azimuths east of this station. These result are consistent with previous studies that show rotation of anisotropy from NE azimuth to an ENE azimuth within the Peitersburg block and Bushveld region as they wrap around the Kaapvaal shield (Silver et al, 2001,2004). This suggests the collisional events at the western and northern boundaries of the Kaapvaal craton produce some type of deformation, but only at its edges.

Fast directions at MOPA, located at the eastern edge of the Pietersburg block, indicate significantly different fast directions of NE-SW. The eastern back-azimuth of shear-wave splitting arrivals to MOPA suggests these events may sample the eastern coast and continental shelf of South Africa and is consistent with APM. The contrast between ENE splits in the Kaapvaal shield and NNE anisotropy on the eastern continental boundary is exemplified by two splitting measurements at CNG, which have a ENE fast direction that samples the shield west of CNG and a N-S fast direction for arrivals east of this station. Ray paths from the east sample the offshore lithosphere producing N-S trending fast directions that are consistent with fast directions produced in a region that contains transform faults.

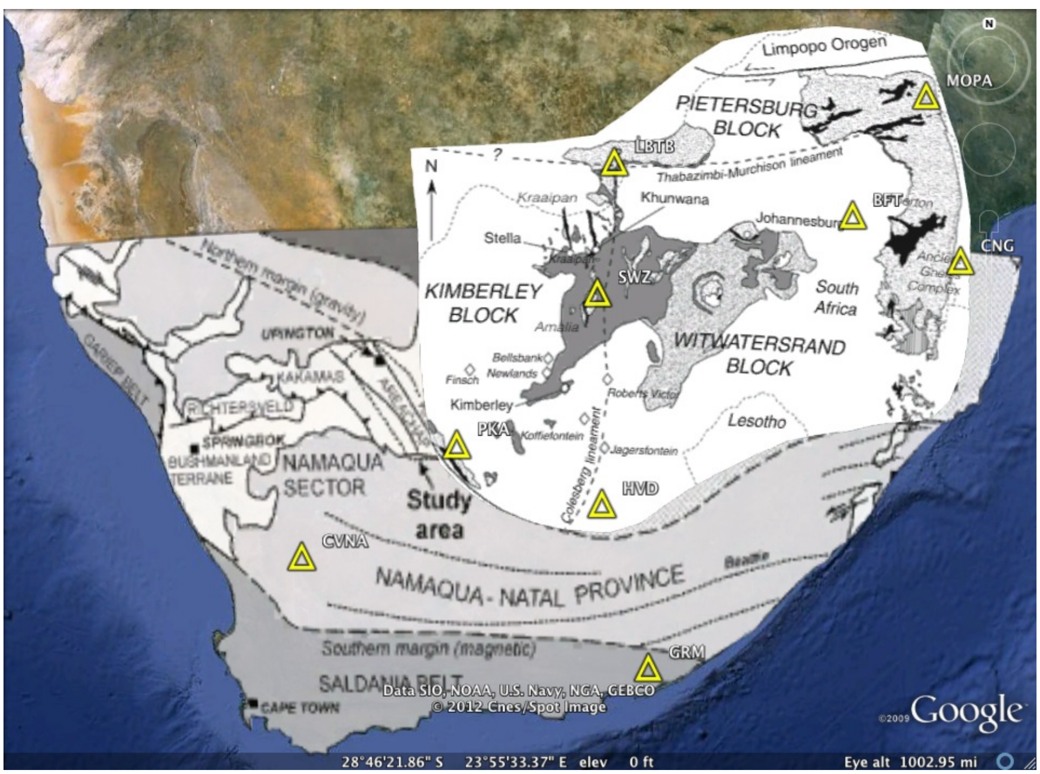

Figure 9: Geological map and tectonic boundary of the Kaapvaal craton (adapted after Schmitz et al., 2004).

4.2.4 Southern Africa

4.2.4.1 Namaqua-Natal Province

Studies of the continental assembly of the Khalari craton (Jacobs et al., 2008) indicate the presence two accretionary belts south of this craton. The Namaqua belt displays fast directions of NNE in the western region of the mobile belt. This is evident from ray paths that approach CVNA from the SE and ray paths that approach PKA from the SW (Figure 7). The Natal belt identified as the eastern section of this fold belt is only sampled by splitting measurements at HVD. This can be seen from events with back-azimuths greater than 150° (roughly SSE) and small incidence angles (Figure 7), which samples the Natal province. These events display NE-SW fast directions. Two splitting measurements arriving with large incidence angles from the eastern azimuths to HVD are consistent with fault systems along the eastern coastal edge of the Natal province may indicate the fault system extends further west beneath the sedimentary cover.

4.2.4.2 Saldania Belt

Few ray paths sample the saldania belt in this study. At CVNA ray paths coming from the southern back-azimuth may sample the region, which borders namaqua and saldania belt indicating this region has a NNE fast direction. Although station GRM is located in the Saldania belt, all results from this station sample the coastal area east of this station. Ray paths from eastern azimuths display NNE fast directions consistent with APM and eastern azimuthal measurements displayed at MOPA, CNG, and GRM. While ray paths that arrive from the southeast display NW-SE fast directions consistent with previous studies suggesting the presence of a remnant subduction zone (Shirey et al.

2001).

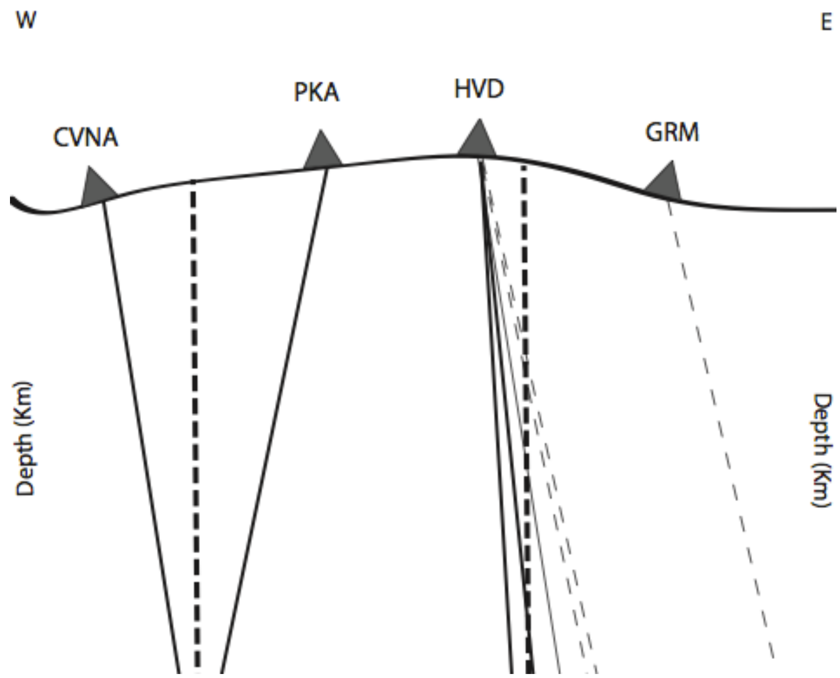

Figure 10: Cross section displaying the ray paths of events recorded at particular stations. Triangles indicate station location in cross section. Black and gray dashed lines show ray path to the given station. Solid dashed displays the boundary separating the two distinctive lithospheric regions.

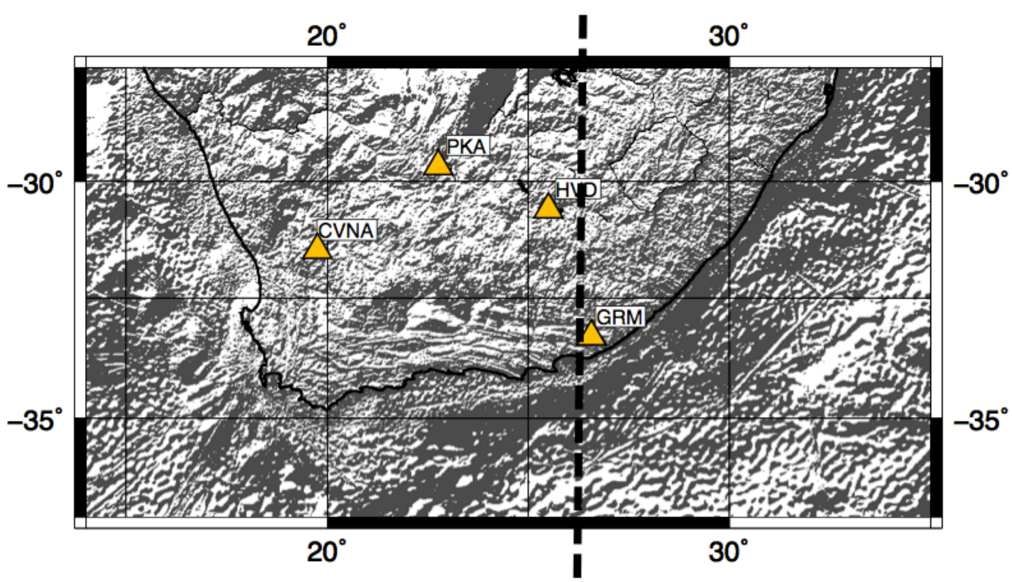

Figure 11: Heavy dashed displays the boundary indicating two distinctive lithospheric regions. Stations are shown by yellow triangles.

This study has shown that delay times produced in mobile belts are significantly larger than delay times within cratons. Splitting results that have fast directions that are parallel to shear zones, produce splitting results that correlate with the least principal stress direction of shear causing anisotropy to wrap around stable cratons. This suggests mobile belts are active processes that continue to deform material. The majority of measurements within mobile belts consistently align and mimic the axis of shear. Based on the results presented in this paper I conclude that seismic anisotropy in mobile belts around world will present splitting directions that mimic the axis of shear.

Chapter 5 Conclusions

5.1 Conclusion

Seismic anisotropy across the continent is not uniform and shows significant variation across tectonic boundaries. While mantle flow and lithospheric deformation attributed to absolute plate motion (N 50° E), may be consistent with several geologic regions of Africa; this simple model cannot explain many of our observations. The most striking observation is the difference in anisotropic values produced in cratons versus mobile belts. We distinguish measurements within continental cratons versus splitting measurements in mobile belts. We averaged results from this study (West African, Congo and Kaapvaal cratons) as well as previous splitting results from the Kaapvaal (Silver et al., 2001) and Tanzanian (Walker et al., 2004) cratons. The delay times averaged over the cratonic regions is 0.67 s +/- 0.136 s and are significantly smaller than delay times observed in mobile belts of 1.4 s +/- 0.074 s. The delay times in the mobile belts are more than twice as large as values produced in the cratonic regions. The small values of anisotropy in the craton may indicate two possible scenarios. In the simplest case, a single layered model may exist where there is a uniform yet a small amount of anisotropy in the cratonic lithosphere and no significant anisotropy in the sub-lithosphere. In the more complex case, a two layer model may exist in the cratonic lithosphere with anisotropy in one direction and in the sub-lithosphere displaying anisotropy in a direction orthogonal to the layer above. In this case vertically traveling SKS phases will integrate these layers and produce reduced delay times at the surface. We consider these two possible scenarios below.

In the Kaapvaal craton the dominant azimuthal direction of splitting is NE-SW and is sub-parallel to APM, with average delay times of 0.67 s that are consistently small over the region (Silver et al. 2004, and this study). If plate motion produces alignment in the sub-lithospheric mantle, anisotropy in these two layers should multiply and produce large split times at the surface. This discounts the two layer model as the combined anisotropy in the lithosphere and sub-lithosphere is very small. This suggests that the slow motion of the African plate may only produce a minimal degree of mineral alignment in the mantle. Previous seismic tomography images have identified the base of the lithosphere in the Kaapvaal craton at ~200 km (Li and Burke, 2006). If any or all the anisotropy we observe is accommodated within the cratonic lithosphere it must also be small.

In the Tanzanian craton, anisotropy from Rayleigh wave tomography and shear-wave splitting show consistent fast directions of NW-SE (Weeraratne et al.,2001; Walker et al., 2004). Average splitting results within the craton are 0.49 s +/- 0.20 and are small. Since absolute plate motion is in the NE-SW direction and opposes this fast direction, this suggests the two layer model may be valid and responsible for the small delay times in the Tanzanian craton. However, the dispersive effects of horizontally traveling surface waves provide depth resolution of azimuthal anisotropy that indicates this uniform direction of NW-SE anisotropy is accommodated in the upper 120 km (Weeraratne et al., 2001). This points to the simpler single layer model and implies anisotropy is found predominately in the lithosphere with little contribution from the sublithosphere.

In both cases the single layer model is supported by the seismic data and plate motion of Africa. Our results suggest that remnant anisotropy is present in the cratonic lithosphere and is the chief contributor to seismic anisotropy measurements for both SKS and surface wave anisotropic phases in cratonic regions. Anisotropy was likely frozen into the Kaapvaal craton when it formed as part of the continent UR (Rogers ,1996) ~2.5 Ga (see Figure 1A or Appendix Figure A1). The Tanzanian craton was a late addition to the continent Atlantica ~2 Ga (Rogers 1996, Jacob 2008). Anisotropic fabric may have developed within Tanzania when it accreted onto the eastern edge of Atlantica (see Figure 1B). This may indicate the slow velocity of the African plate produces very little anisotropy in the sub-lithosphere. Coverage of cratonic regions across the continent is not extensive and therefore additional coverage may be warranted in future studies.

To explain the difference between anisotropy produced on cratonic lithosphere and mobile belts, I compare the variation in their physical properties. Cratons have experienced multiple cycles of subduction, collision, and repeated melting (e.g. Durrhiem et al., 1994) in their lengthy history, consequently creating a depleted lithospheric fabric (Jordan, 1978). The occurrence of depletion and dehydration (Jung and Karato, 2001) within a craton from convergent events produces stronger, less dense, buoyant, and stable lithosphere (Lee and Rudnick, 2007, Schutt and Lesher, 2006) that is resistant to deformation during collisional events. Mobile belts by contrast are composed of minerals such as garnet lherzolites (Jordan, 1978; Durrhiem et al., 1994), are younger in age, more fertile, and have a shorter tectonic history than cratons. During collisional events, cratons may therefore act as stable blocks while strain is accommodated by the weaker mobile belts, producing intense deformation and stronger anisotropy between cratonic regions. Remnant anisotropic fabric may thus be preserved in cratonic lithosphere where it is stored from previous collisional events (Silver, 1996).

5.2 Future work and Projects

Although our study covers a large region of the African continent there is a lack of results provided that sample the interior of cratons in general including the Kaapvaal, Congo and West African cratons. We also suggest future seismic studies to be performed in Guyana, Brazillian, and Sao Francisco cratons in South America. With this proposed study it may be determined whether the NW –SE fabric found in the West African and Congo Cratons is uniform fabric is continuous within other cratonic lithosphere of Atlantica. The Zimbabwe and Kaapvaal cratons along with rift zones located in Eastern and Southern Africa display splitting directions that are parallel to the APM of the continental plate. To distinguish whether or not these splitting values are caused by plate motion or through various tectonic events I propose that a study to be conducted that will use local events to determine which factor is causing the anisotropy.

References

Barruol, G. and W. B. Ismail, Upper mantle anisotropy beneath the African IRIS and Geoscope stations, *Geophysical Journal International*,*146* , 549-561, 2001

Barruol, G. and R. Hoffmann, Upper mantle anisotropy beneath the Geoscope stations, *Journal of Geophysical Research*, *104,* 10757-10773,1999

Begg, G.C., W.L. Griffin, L.M. Naptapov, S.Y. O'Reily, S.P. Grand, C.J. O'neil, J.M.A. Hronsky, Y. Poudjom, C.J. Swain, T. Deen and P. Bowden, The lithospheric architecture of Africa; Seismic tomography, mantle petrology, and tectonic evolution, *The Geological Society Of America, 5*, doi: 10.1130/GES00179.1, 23-50, 2009

Behn, M. D., C.P. Conrad, and P.G. Silver, Detection of upper mantle flow associated with the African Superplume, *Earth and Planetary Science Letters, 224*, doi:10.1016/j.epsl.2004.05.026, 259-274, 2004

Burke, K., The African Plate, *South African Journal of Geology, 99,* 339-410,1996

DeMets, C., R.G. Gordon, D. F. Argus and S. Stein, *Geophysical Research Letters, 20*,

Durrheim, D.J. and W.D. Mooney, Evolution of the Precambrian Lithosphere: Seismological and geochemical constraints, *Journal of Geophysical Research,99*, 15,359-15,374,1994

Fouch, M. J., James, D.E., VanDecar, J. C., van der Lee, S., the Kaapvaal seismic group, Mantle seismic structure beneath the Kaapvaal and Zimbabwe Cratons, *South African journal of geology*, 107, 33-44, 2004

Fouch, M. J., Rondenay, S., Seismic anisotropy beneath stable continental interiors, *Physics of the Earth and Planetary Interiors*, 158, 292-320, 2006

Fouch, M. J., Silver, P. G., Bell, D. R., and Lee, J. N., Small-scale variations in seismic anisotropy near Kimberley, South Africa*, Geophysics Journal International*, 157, 764-774, 2004.

Gao,S., P.M. Davis, H. Liu, P.D. Slack, A.W. Rigor, Y.A. Zorin, V.V. Mordvinova, V.M. Kozhevnikov and Logatchev, SKS splitting beneath continental rift zones, J. *Geophysical Research Letters, 102*, B01858 doi: 10.1029/2002GLO16616, 22781-22797,1997

Gashawbeza, E. M., S. L. Klemperer, A. A. Nyblade, K. T. Walker, and K. M. Keranen, Shear-wave splitting in Ethiopia: Precambrian mantle anisotropy locally modified by Neogene rifting, *Geophysical Research Letters*, *31*, doi: 10.1029/2004GL020471, 2004.

Hansen, S., S. Schwartz, A. Al-Amri, and A. Rodgers, 2006, Combined plate motion and density-driven flow in the asthenosphere beneath Saudi Arabia: Evidence from shear-wave splitting and seismic anisotropy, *Geology, 34*, doi:10.1130/G22713.1869-872, 2006.

Jacobs, J. Pisarevsky, S., Thomas, R. J., Becker, T., The Kalahari craton during the assembly and dispersal of Rodinia, *Precambrian research*, 160, 142-158, 2008

James, D. E., Fouch, M. J., VanDecar, J. C., van der Lee, S., the Kaapvaal seismic group, *Geophysical research letters*, 28, 2485-2488, 2001

Jelsma, H., Barnett, W., Richards, S., Lister, G., Tectonic setting of kimberlites, *Lithos*,

112S, 155-165, 2009
Jordan, T. H., Composition and development of the continental tectosphere, *Nature*, 274, 544-548, 1978
LaBarre, E. A., Davis, T.L. and Benson, R.D., Finding the sweet spot, *www.epmag.com,* 2008
Lee, C. T., Rudnick, R. L., McDonough, W. F., Horn, I., Petrologic and geochemical investigation of carbonates in peridotite xenoliths from northeastern Tanzania, Contrib Mineral Petrol, 139, 470-484, 2000
Li, A., Burke, K., Upper mantle structure of southern Africa from Rayleigh wave tomography, *Journal of Geophysical research*, 111, B10303, 2006\
Marshak, S. Essentials of Geology,second edition,2007
Minex, Greenland mineral exploration newsletter, Greenland is ready to join the new diamond rush in the Artic,Geological survey of Denmark and Greenland, 2002
Nguuri T.K., J. Gore, D. E. James, S. J. Webb, C. Wright, T. G. Zengeni, O. Gwavava, J. A. Snoke, and Kaapvaal Seismic Group, Crustal structure beneath southern Africa and its implications for the formation and evolution of the Kaapvaal and Zimbabwe cratons, , *Geophysical Research Letters, 28*, 2501-2504, 2001.
Pasyanos, M. E., and A. A. Nyblade, 2007, A top to bottom lithospheric study of Africa and Arabia, *Tectonophysics, 444*, doi: 10.1016/j.tecto.2007.07.008,27-44, 2007.
Richardson, S. H., Shirey, S. B., Harris, J. W., Carlson, R. W., Archean subduction recorded by Re-Os isotopes in eclogitic sulfide inclusions in Kimberley diamonds, Earth and Planetary Science Letters, 191, 257-266, 2001
Ritsema. J, Jan van Heijst, H., Woodhouse, J. H., Complex Shear Wave Velocity Structure Imaged Beneath Africa and Iceland, Science, 286, 1925-1928,1999
Rogers, J.J.W., A History of Continents in the Past Three Billion Years, *The Journal of Geology, 104,* 91-107,1996
Rychert, C. A., Shearer, P. M., A Global View of the Lithosphere-Asthenosphere Boundary, Science, 324, 495-498, 2009
Sain, K., Energy Partitioning of seismic waves, *encyclopedia of solid earth geophysics.* P.291, 1989
Savage, M., K., Seismic anisotropy and mantle deformation: what have we learned from shear wave splitting?, *Reviews of Geophysics, 37*, 65-106,1999
Schmitz, M.D., Bowring, S. A., de Wit, Maarten J., Gartz, V., Subduction and terrane collision stabilize the western Kaapvaal craton tectosphere 2.9 billion years ago, Earth and Planetary Science Letters, 222, 363-376, 2004
Schutt, D.L., and Lesher, C.E., Effects of melt depletion on the density and seismic velocity of garnet and spinel lherzolite, Journal of geophysical Research, 111, 2006
Shirey, S.B., J.W. Harris, S.H. Richardson, M.J. Fouch, D. E. James, P. Cartigny, P. Deines and F. Viljoen, Diamond Genesis, Seismic Structure, and Evolution of the Kaapvaal-Zimbabwe Craton, *Science*, *297*, 1683-1687, 2002
Silver, P. G., *Seismic anisotropy beneath the continents: Probing the depths of geology,* Ann Rev. Earth. Planet. Sci., 24, 385-432, 1996.
Silver, P. G., and W. W. Chan, Shear wave splitting and subcontinental mantle deformation, *Journal Geophysical Research, 96*, B10, 16,429-16,454, 1991.
Silver, P. G., M.J. Fouch, S. S. Goa and M. Schmitz, Seismic anisotropy, mantle fabric,

and the magmatic evolution of Precambrian southern Africa, South African *Journal Of Geology,107,* 45-58, 2004

Silver, P. G., Gao, S. S., Liu, K.H. and the Kaapvaal Seismic Group, *Mantle deformation beneath southern Africa*, Geophysical Research Letters, 28, 2493-2496, 2001.

Stankiewicz, J., S. Chevrot, R. D. van der Hilst, M. J. de Wit, Crustal thickness, discontinuity depth, and upper mantle structure beneath southern Africa: constraints from body wave conversions, *Physics of the Earth and Planetary Interiors, 130,* 235-251, 2002.

Stein,S., Wysession, M., An Introduction to seismology, Earthquakes, and Earth Structure, Blackwell Publishing, 2003.

Walker, K. T., A. A. Nyblade, S. L. Klemperer, G. H. R. Bokelmann, and T. J. Owens, On the relationship between extension and anisotropy: Constraints from shear wave splitting across the East African Plateau, *Journal of Geophysical Research, 109*, B08302 doi: 10.1029/2003JB002866, 2004.

Weeraratne, D., D.W. Forsyth, K. M. Fischer, and A .A. Nyblade, Evidence for an upper mantle plume beneath the Tanzanian craton from Rayleigh wave tomography, *Journal of Geophysical Research, 108* (B9), 2427, doi:10.1029/2002JB002273, 2003.

Woods, J., Guth, A., East Africa's Great Rift Valley: A complex Rift System, *Geology.com*

Wüstefeld, A., G. Bokelmann, C. Zaroli, and G. Barruol, SplitLab: A shear-wave splitting environment in Matlab, *Computers & Geosciences, 34,* p. 515-528, 2008.

Wüstefeld, A. and Bokelmann, G., Null detection in shear-wave splitting measurements, *Bull. Seism. Soc. Am., 97*, 4, 1204-1211, doi: 10.1785/0120060190, 2007.

Appendix

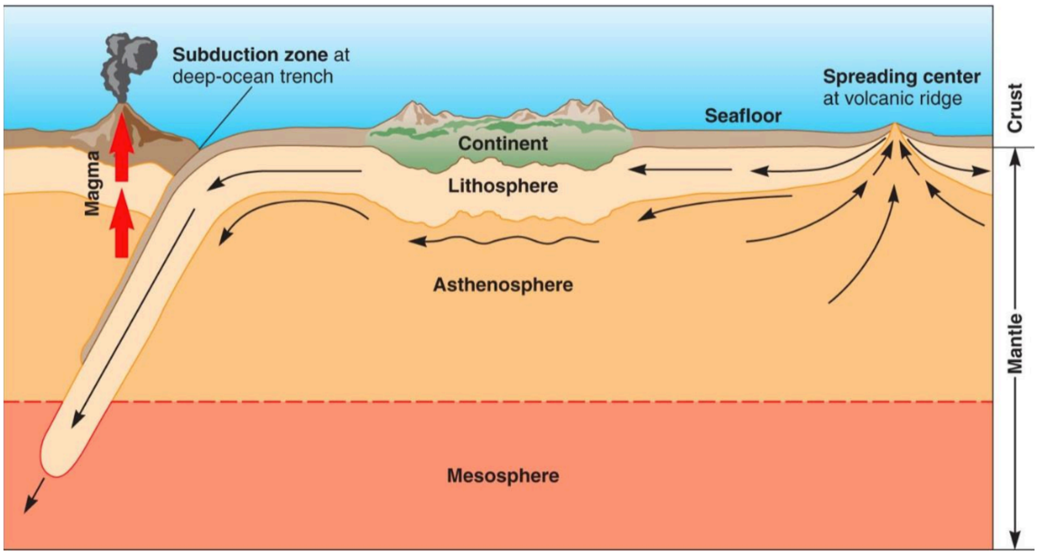

Figure A1: Propagation of plates in subduction zone. As plates propagate in a particular direction, they drag material below consequently producing alignment in the upper mantle (Marshak, 2007).

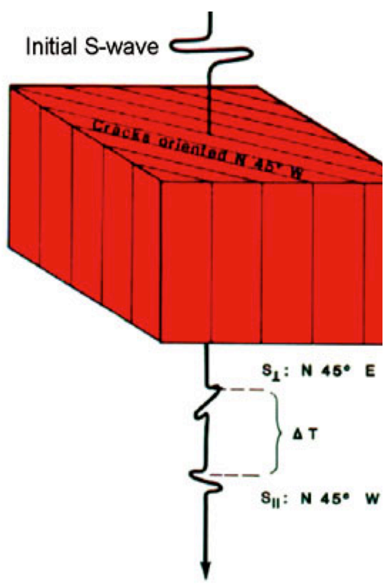

Figure A2: Depiction of a shear wave passing through a medium with mineral alignment in a given direction (LaBarre et al.,2008).

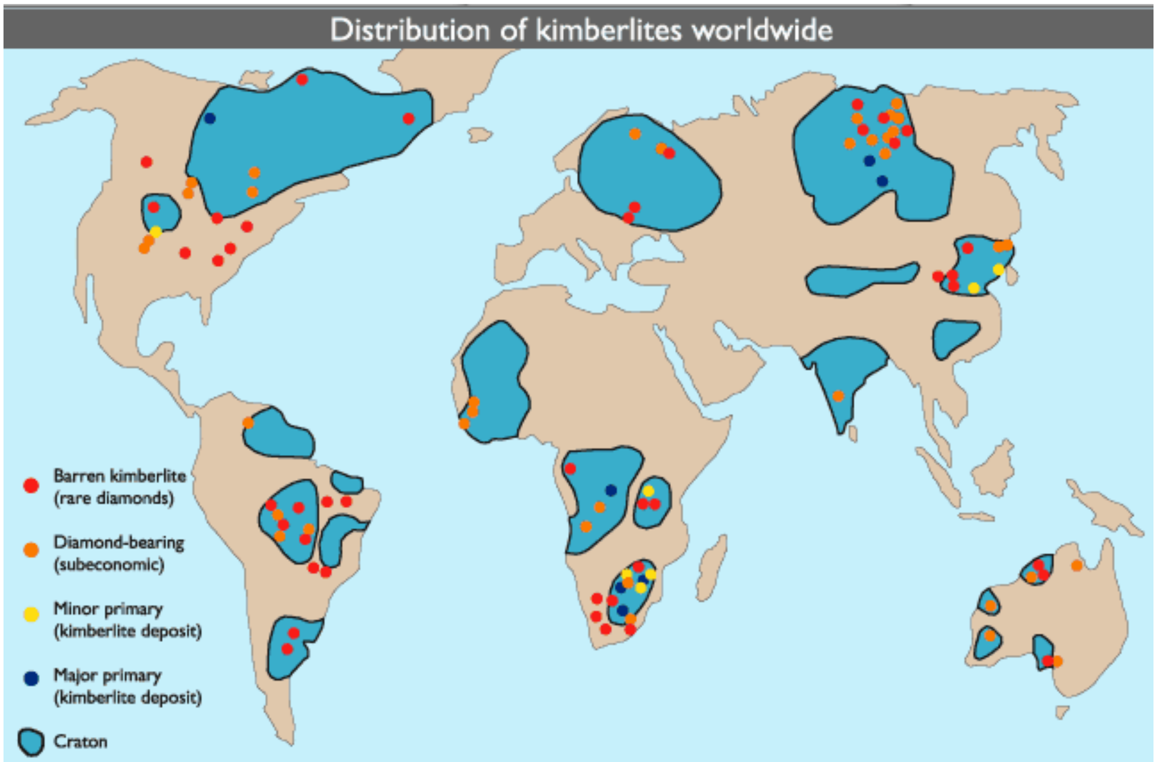

Figure A3: Distribution of cratons throughout the world. Cratons are indicated by enclosed blue regions (Minex, 2002).

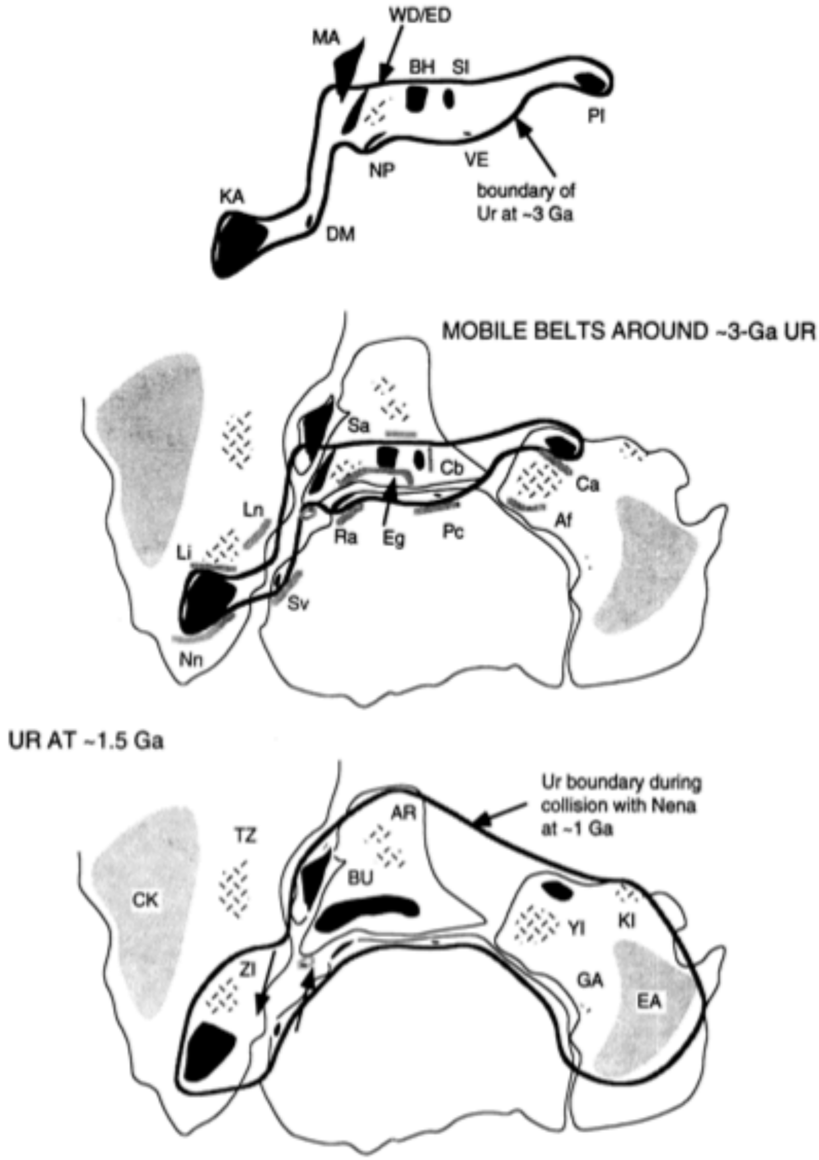

C)

Figure A4: Displays the growth of UR. Originally UR was comprised of Pilbara craton, Kaapvaal craton, Bhandara craton and the Singhbhum craton. Through the collision of additional fragments and the addition of mobile belts the continent grew into figure C, (Rogers, 1996).

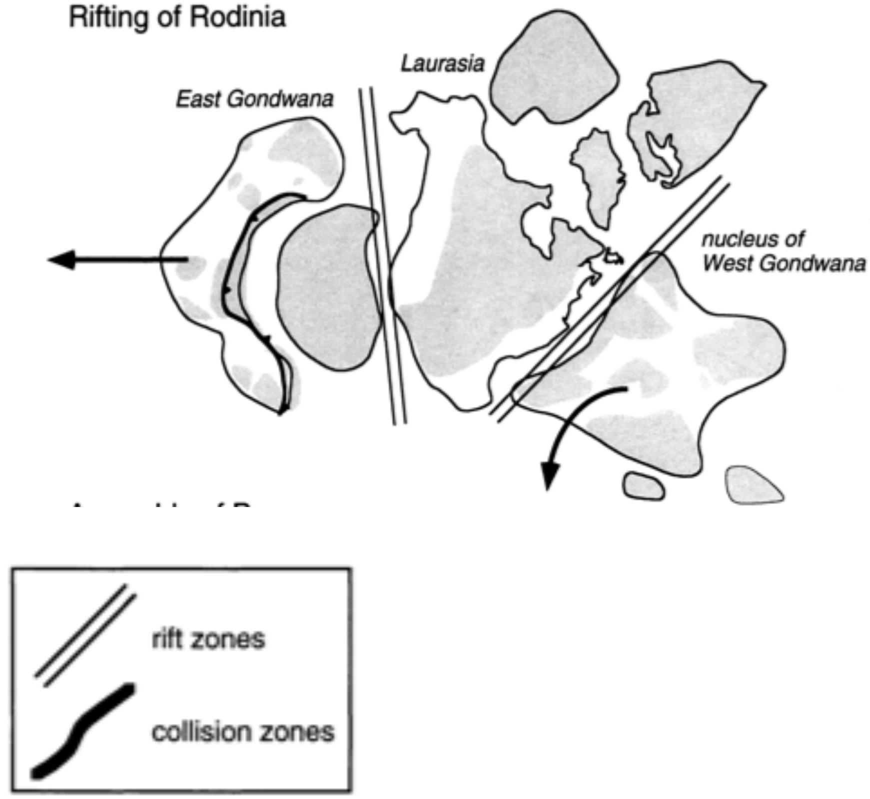

Figure A5: Displays two large rifts throughout the continent of Rodinia. Double lines represent rift zones (Rogers, 1996).

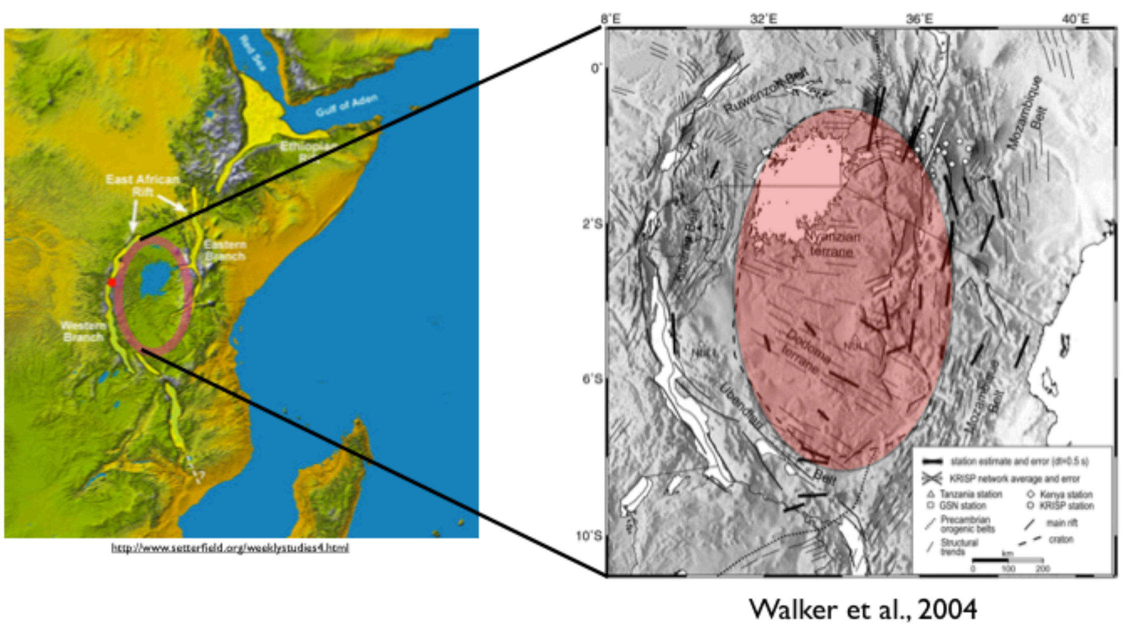

Figure A6: Results for study done in the Tanzanian craton (Walker et al. 2004). The dominant fast directions from study done in the interior of the Tanzanian craton are NW-

SE (Woods and Guth, 2005).

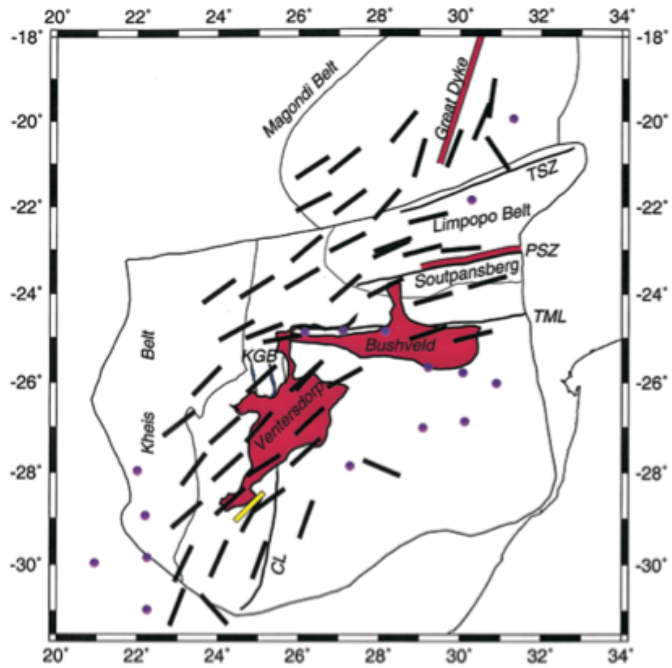

Figure A7: Results for study done in the Kaapvaal craton (Silver et al. 2004). Most observations in the Kaapvaal experiment are found to occur in the shear zone.

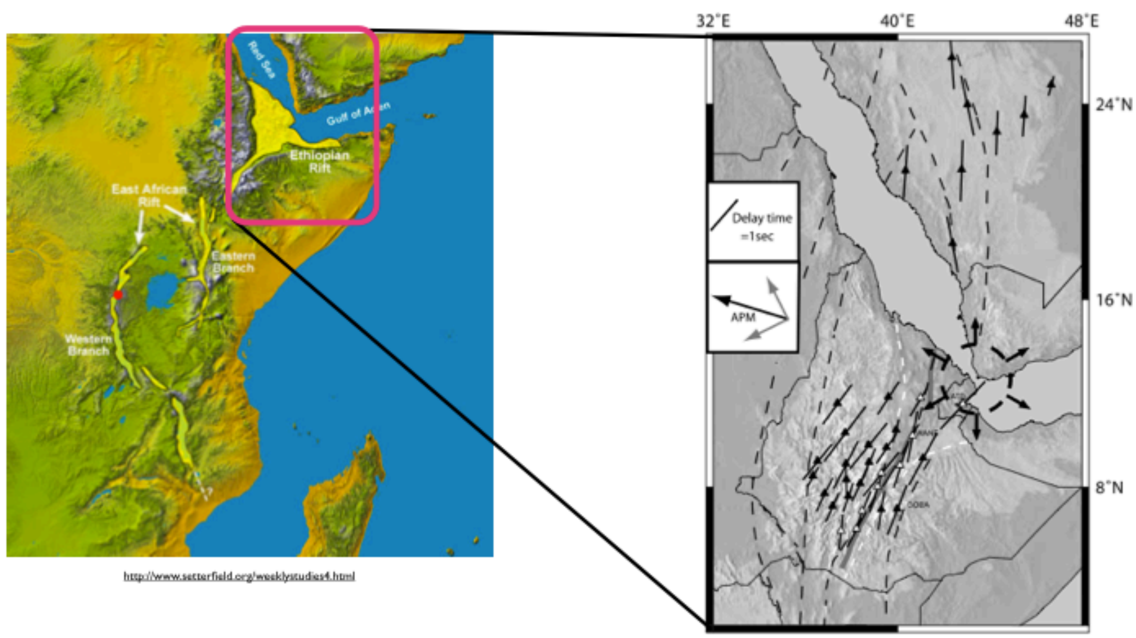

Figure A8: Study done in the main Ethiopian rift system (Gashawbeza et al., 2004). Shear wave splitting measurement in the rift system is NE-SW (Woods and Guth, 2005).

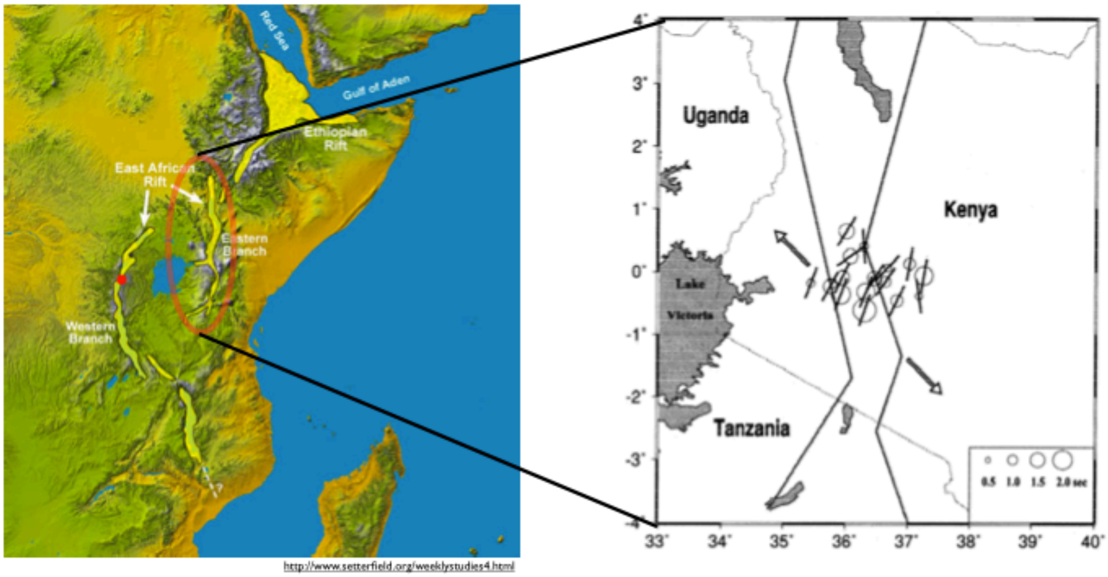

Figure A9: Shear-wave splitting study done in the Eastern Branch of the East African Rift. Fast directions are sub-parallel to rift axis (Gao et al., 1997 and Woods and Guth, 2005).

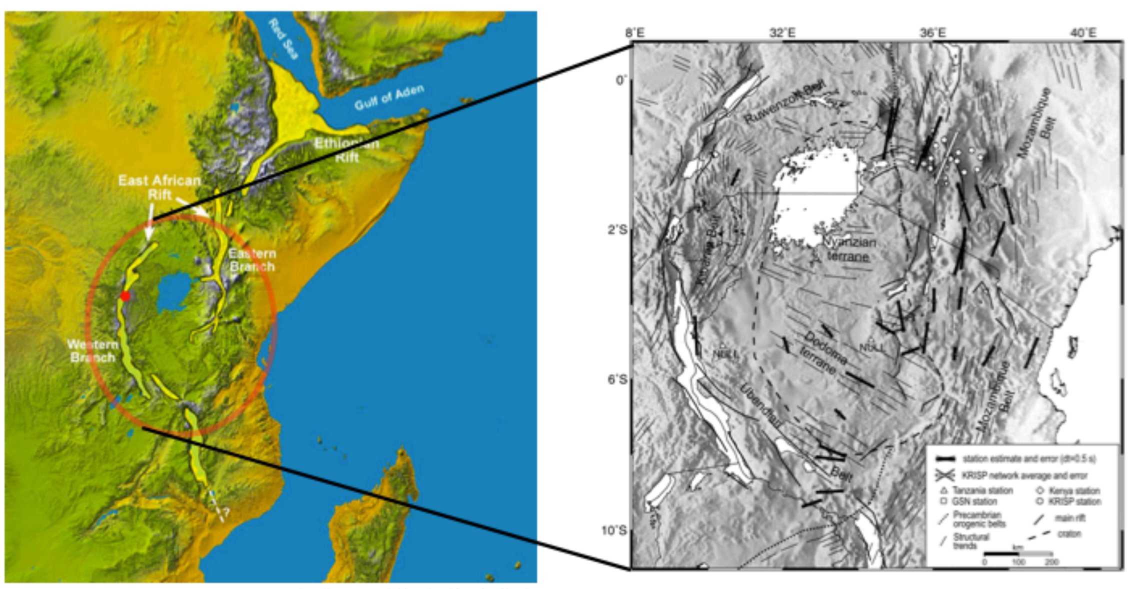

Figure A10: Shear-wave splitting study done surrounding the Tanzanian craton. Fast directions in rift zones at the perimeter wrap around the Tanzanian craton (Walker et al. 2004 and Woods and Guth, 2005).

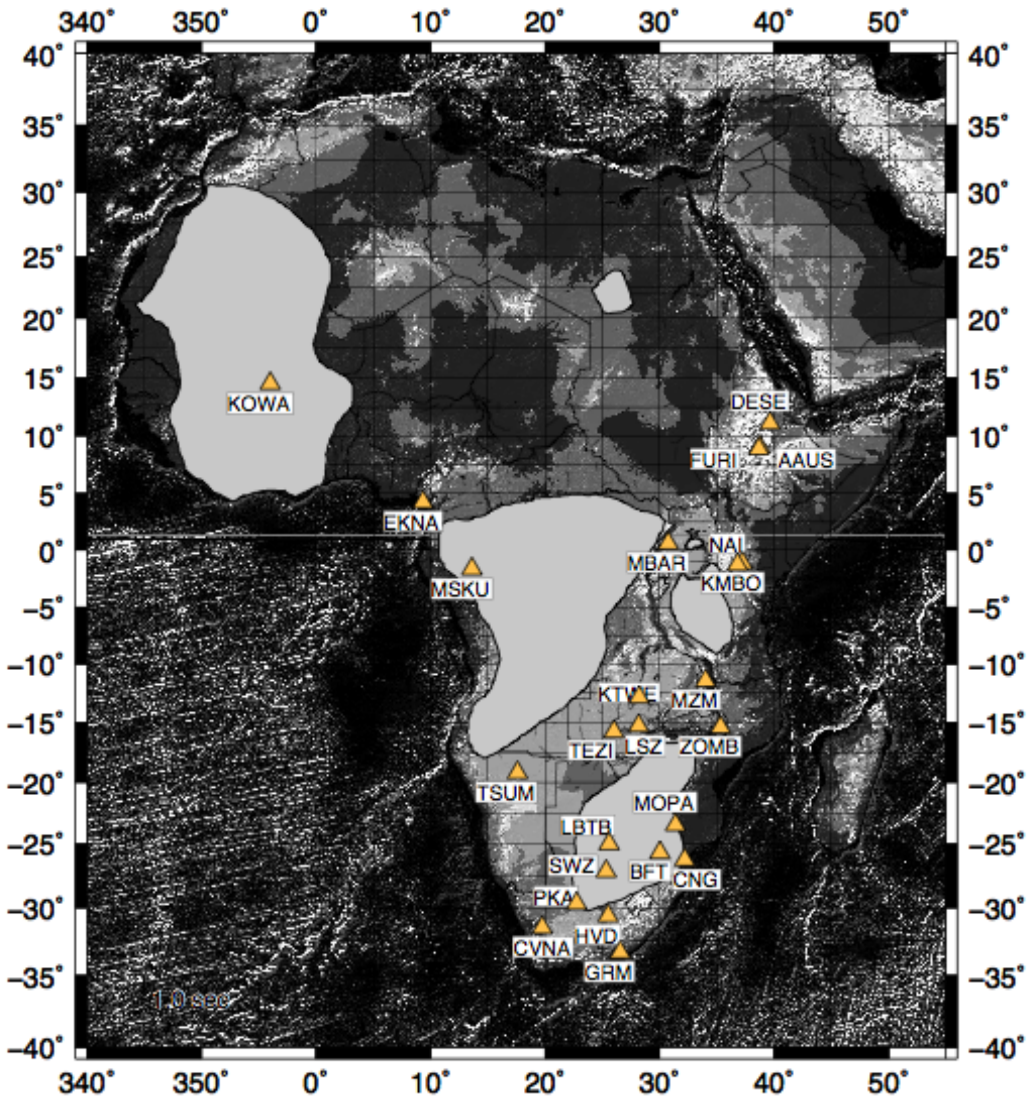

Figure A11: Shows station location in relation to the African continent. Yellow triangles represent stations location. Gray enclosed regions represent cratons.

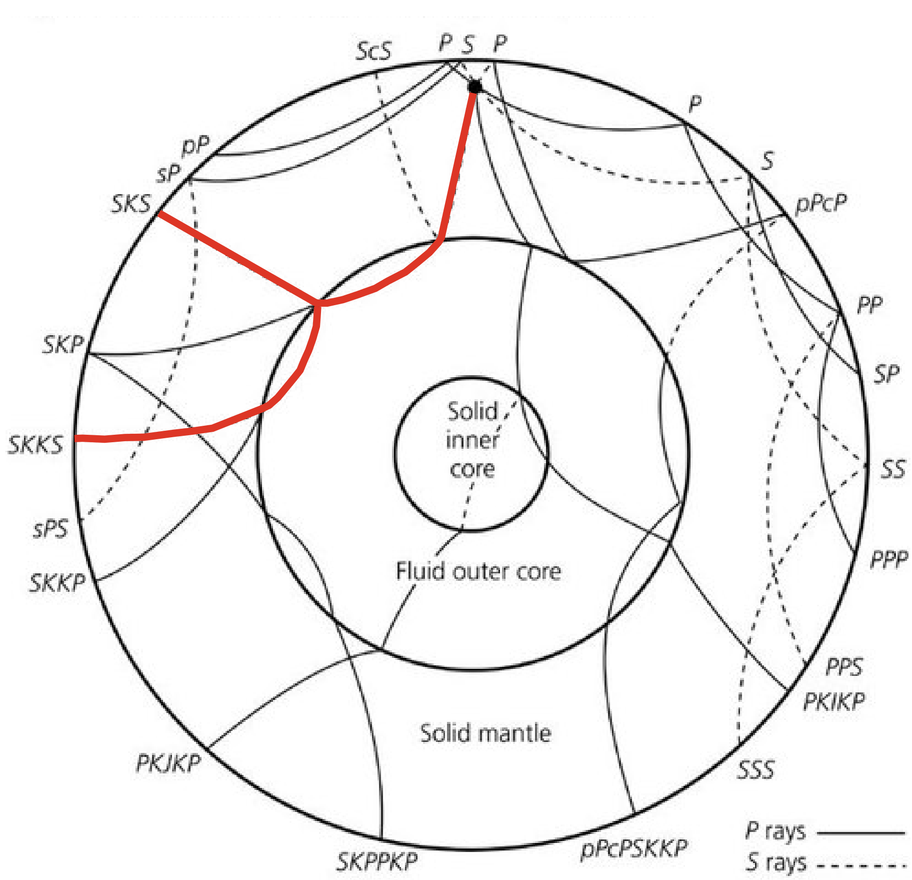

Figure A12: Highlighted in red are the SKS and SKKS phases. These phases are particularly beneficial because they only record anisotropy present in the mantle on the receiver side (adapted after Stein and Wysession, 2003).

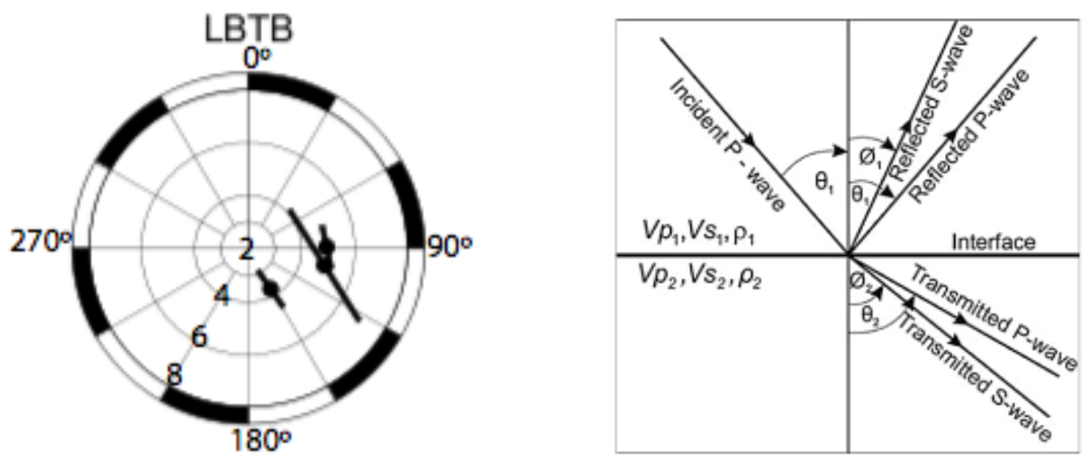

Figure A13: Left: The circular plot displays Back azimuth, ray parameter and fast direction. The arrival azimuth is displayed in map view from 0°-360°. Fast direction is indicated by the black bar (Sain, 1989).